TU Delft

Delft University of Technology

NEEDS, TRENDS and ADVANCES IN INORGANIC SCINTILLATORS

Dujardin, C.; Auffray, E.; Bourret, E.; Dorenbos, P.; Lecoq, P.; Nikl, M.; N.Vasil'ev, A.; Yoshikawa, A.; Zhu, R.

DOI
10.1109/TNS.2018.2840160

Publication date
2018

Document Version
Final published version

Published in
IEEE Transactions on Nuclear Science

Citation (APA)
Dujardin, C., Auffray, E., Bourret, E., Dorenbos, P., Lecoq, P., Nikl, M., N.Vasil'ev, A., Yoshikawa, A., & Zhu, R. (2018). NEEDS, TRENDS and ADVANCES IN INORGANIC SCINTILLATORS. *IEEE Transactions on Nuclear Science*, *65*(8). https://doi.org/10.1109/TNS.2018.2840160

Important note
To cite this publication, please use the final published version (if applicable).
Please check the document version above.

Copyright
Other than for strictly personal use, it is not permitted to download, forward or distribute the text or part of it, without the consent of the author(s) and/or copyright holder(s), unless the work is under an open content license such as Creative Commons.

Takedown policy
Please contact us and provide details if you believe this document breaches copyrights.
We will remove access to the work immediately and investigate your claim.

This work is downloaded from Delft University of Technology.
For technical reasons the number of authors shown on this cover page is limited to a maximum of 10.

Needs, Trends, and Advances in Inorganic Scintillators

C. Dujardin, E. Auffray, E. Bourret-Courchesne, P. Dorenbos, P. Lecoq, M. Nikl, A. N. Vasil'ev, A. Yoshikawa, and R.-Y. Zhu

***Abstract*— This paper presents new developments in inorganic scintillators widely used for radiation detection. It addresses major emerging research topics outlining current needs for applications and material sciences issues with the overall aim to provide an up-to-date picture of the field. While the traditional forms of scintillators have been crystals and ceramics, new research on films, nanoparticles, and microstructured materials is discussed as these material forms can bring new functionality and therefore find applications in radiation detection. The last part of the contribution reports on the very recent evolutions of the most advanced theories, methods, and analyses to describe the scintillation mechanisms.**

***Index Terms*— Fast timing, high energy physics (HEP), homeland security, inorganic scintillator, medical imaging, scintillation.**

I. Introduction

SCINTILLATING materials are currently widely used in many detection systems addressing different fields, such as medical imaging, homeland security, high energy physics (HEP) calorimetry, industrial control, and oil drilling exploration. Among them, inorganic materials occupy a large part of the research activity and the market share, estimated at about $350 million in 2015. More than one century after the first use of a scintillating material, the research is still very active as detector technologies are progressing, functionalities and performances of ionizing radiation systems are changing, and material synthesis methods and related knowledge have been greatly improved and extended. Theory and modeling of scintillation mechanisms have significantly been improved since that time. The purpose of this contribution is to present the very recent advances and trends in inorganic scintillation science. A particular focus is given on emerging fields of interest related to scintillation regarding materials. Of course, it is not currently expected that the presented materials will soon be the substitutes for the widely used compounds, such as NaI:Tl, CsI:Tl, and Lu_2SiO_5:Ce, but it is believed that the described areas have potential to outperform some of the quality criteria as compared with the well-established compounds. As described latter, some of these quality criteria are well connected with the emerging needs requiring particular ionization radiation response.

The discovery of new scintillators has been an important subject of research for years. Two main events have largely contributed to these successful discovery efforts: the advent of the "Crystal Clear Collaboration" (CCC) [1] back in 1990 headed by CERN and the SCINT conference creation in 1992 (originally called Crystal 2000) [2]. In the past decades, research on the scintillating materials was dominated by the needs for positron emission tomography (PET) and high energy calorimetry. Most of the applications using scintillating materials were based on the density, scintillation, and time response performances. Based on these three parameters, an impressive number of heavy cation (particularly lutetium)-based hosts doped with Ce^{3+} or Pr^{3+} have been investigated. Some attempts are currently made with hafnium- or thallium-based materials. Homeland security requires widely deployed detectors for γ-ray spectroscopy. Decay time is less critical but a strong requirement regarding the energy resolution emerged, and Eu^{2+}-doped halides have been extensively developed in this framework.

Nowadays, the requirements in terms of performance are more and more demanding. Time-of-flight (TOF) applications ask for sub-100 ps time resolution; for homeland security, energy resolution down to 2%–3% for large crystals is desired and neutron/γ discrimination is always wanted. Fast neutron

Manuscript received January 29, 2018; revised April 9, 2018; accepted April 11, 2018. Date of publication May 24, 2018; date of current version August 15, 2018. This work was supported in part by the European Research Council for the ERC Advanced under Grant TICAL 338953, in part by the EC Project H2020-TWINN-2015 under Grant 690599 (ASCIMAT), in part by the European Union Horizon 2020 Program under Grant Agreement 644260 (INTELUM), in part by the European Union under the COST Action TD under Grant 1401 (FAST), and in part by the Crystal Clear Collaboration. The work of E. Bourret-Courchesne was supported by the U.S. Department of Energy/NNSA/DNN Research and Development carried out at Lawrence Berkeley National Laboratory under Contract AC02-05CH11231 (this funding does not constitute an express or implied endorsement on the part of the U.S. Government). The work of R.-Y. Zhu was supported by the U.S. Department of Energy, Office of High Energy Physics Program under Award DE-SC0011925.

C. Dujardin is with the Université de Lyon, Université Claude Bernard Lyon 1, CNRS, Institut Lumière Matière UMR 5306, F-69622 Villeurbanne, France (e-mail: christophe.dujardin@univ-lyon1.fr).

E. Auffray and P. Lecoq are with the European Organization for Nuclear Research (CERN), CH-1211 Geneva, Switzerland (e-mail: etiennette.auffray@cern.ch; paul.lecoq@cern.ch).

E. Bourret-Courchesne is with the Lawrence Berkeley National Laboratory, Berkeley, CA 94720 USA (e-mail: edbourret@lbl.gov).

P. Dorenbos is with the Faculty of Applied Sciences, Delft University of Technology, 2629JB Delft, The Netherlands (e-mail: p.dorenbos@tudelft.nl).

M. Nikl is with the Institute of Physics of the Czech Academy of Science, Prague 16200, Czech Republic (e-mail: nikl@fzu.cz).

A. N. Vasil'ev is with the Skobeltsyn Institute of Nuclear Physics, Lomonosov Moscow State University, 119991 Moscow, Russia (e-mail: anvasiliev@rambler.ru).

A. Yoshikawa is with the Institute for Materials Research, Tohoku University, Sendai 980-8577, Japan (e-mail: yoshikawa@imr.tohoku.ac.jp).

R.-Y. Zhu is with the California Institute of Technology, Pasadena, CA 91125 USA (e-mail: zhu@hep.caltech.edu).

Color versions of one or more of the figures in this paper are available online at http://ieeexplore.ieee.org.

Digital Object Identifier 10.1109/TNS.2018.2840160

0018-9499 © 2018 IEEE. Translations and content mining are permitted for academic research only. Personal use is also permitted, but republication/redistribution requires IEEE permission. See http://www.ieee.org/publications_standards/publications/rights/index.html for more information.

detection is also needed. In high energy calorimetry, strategies to add the electromagnetic and nonelectromagnetic particle discrimination functionalities are developed. Bolometry for rare events search, such as double β decay or weakly interactive massive particle as candidate for dark matter, requires extraordinarily radio-pure scintillating crystal operating at a few mK. As a result, the current and probably future research tends toward the development of very specialized scintillators. Designs of detector include various scintillator types to combine the best performance of each start to appear. Hybrids or metamaterials are a new tendency. Discovery of a new material has a different meaning than in the past, since, now, each performance parameter has to be optimized. As an illustration, codoping a known material changes drastically its performances as will be described latter. Nanoparticles are also more and more developed and studied for scintillating applications. Apart from their composition, changing their shape can give rise to a new material. It generally refers more to light collection rather than to light production, thus playing an important role for imaging applications. Of course, most of the described field of interest are far to be mature, and some first published results may need to be further validated and/or reproduced, and this paper invites the scintillation research community to do. This paper focuses first on the emerging needs requiring new scintillation performances. A particular attention is given on requirements for nuclear security, ultrafast timing, fast imaging, fast neutron detection, and the new needs for HEP. Consequently, this paper presents recent and very recent new developments, such as codoping, nanomaterials, eutectics, and crystalline fibers, that can, in addition to the more mature technologies, address some of the required criteria. All these developments being connected to the knowledge of the scintillation mechanisms, it is crucial to describe the recent progress of these aspects as well.

II. Current Demands

A. Nuclear Security

The uses of detector materials for nuclear security are numerous and varied in scope: direct search, detection, and identification of nuclear materials; contamination zone mapping; materials control and accounting; material diversion detection and unattended monitoring; arms control and treaty verification; countering the threat of nuclear materials smuggling; and so on. These applications have a range of requirements, from small high-performance detectors to large high-efficiency detectors, and also a wide range of production quantities, from a few detectors to hundreds or even thousands and sizes as varied as a few cc to large arrays covering square meter areas. Radiation detector materials are the core sensing technology that drive capabilities and impose limitations. The discovery of new scintillators toward the national security issues has been an important subject of research in the last decade triggered in large part by a significant input of U.S. research funds starting in 2008, as shown in Fig. 1. While the CCC was originally set up to develop scintillator for HEP and latter for medical applications, it has produced a number of new scintillator crystals and has contributed to major advances in fundamental understanding of scintillation applicable to the national security needs. In the last decade, the search for new scintillators for national security was mainly focused on finding the ideal scintillator for gamma spectroscopy with a high light output, a good proportionality, and an energy resolution of about 2% at 662 keV. Since 2008, a high-throughput search for new scintillators [3] mainly focused on halides has unearthed many new scintillators. New scintillators were discovered or improved outside of the traditional binary systems, such as NaI, CsI, and $LaBr_3$. This effort has triggered other large discovery worldwide efforts and papers describing new scintillators have flooded the scintillation literature. Some of those are listed in [4]. Among oxides, the development of garnets of general formula $Ln_3(Al,Ga)_5O_{12}$, where Ln is Y, Gd, or Lu, or some combination of those is significant. The Gd, Al/Ga garnets (GAGG) are now produced with a light output of about 60 000 ph/MeV closing the gap between oxides and the traditionally better halide scintillators. Activated with Ce, the garnets have a superior timing performance but timing is not a major constraint for most of gamma detection applications for national security as long as it does not exceed about 1 μs. The cumulative work on halides demonstrates that most halides designed from the periodic table columns I, II, and III to VI and having a proper bandgap to accept an activator are scintillators. Two new classes of halides have emerged which can be described as mixed halides that are solid solutions of binary halides and the complex halides with defined composition of three or more elements, such as the elpasolites [5]. Excellent scintillators with performance close to the theoretical limit in light output have been discovered or improved (e.g., BaBrI [6], $CsBa_2I_5$ [7], [8], and SrI_2 [9]).

In parallel, a number of advances in the understanding of characteristics/mechanisms that drive scintillator performance have been made. Up to now, these advances have largely not translated to commercial products in part due to barriers to transition from discovery to production. Some issues that typically limit scaling of materials are related to difficult synthesis, poor consistency in performance, and/or an unacceptable production cost, an important factor for large-scale deployment. The lack of clear understanding of the relationships between intrinsic and extrinsic defects in the materials and scintillation precludes a targeted approach to process optimization. For gamma spectroscopy alone, there is still a shortage of scintillators that can be grown easily and reproducibly in size of 2 inch and above maintaining excellent performance and an incomplete understanding of performance-related scintillation mechanisms. The large discovery and development efforts, however, have not been in vain as efforts pulling together the fields of chemistry, materials sciences and engineering, materials physics, and computational sciences have provided major scientific contributions. Some examples are as follows.

- *Use of Innovative Approaches to Material Development:* Advances in materials discovery (screening approaches, experimental and theoretical guided search, and materials informatics), improved synthesis and processing techniques, and development of novel material media (e.g., amorphous materials and transparent ceramics).

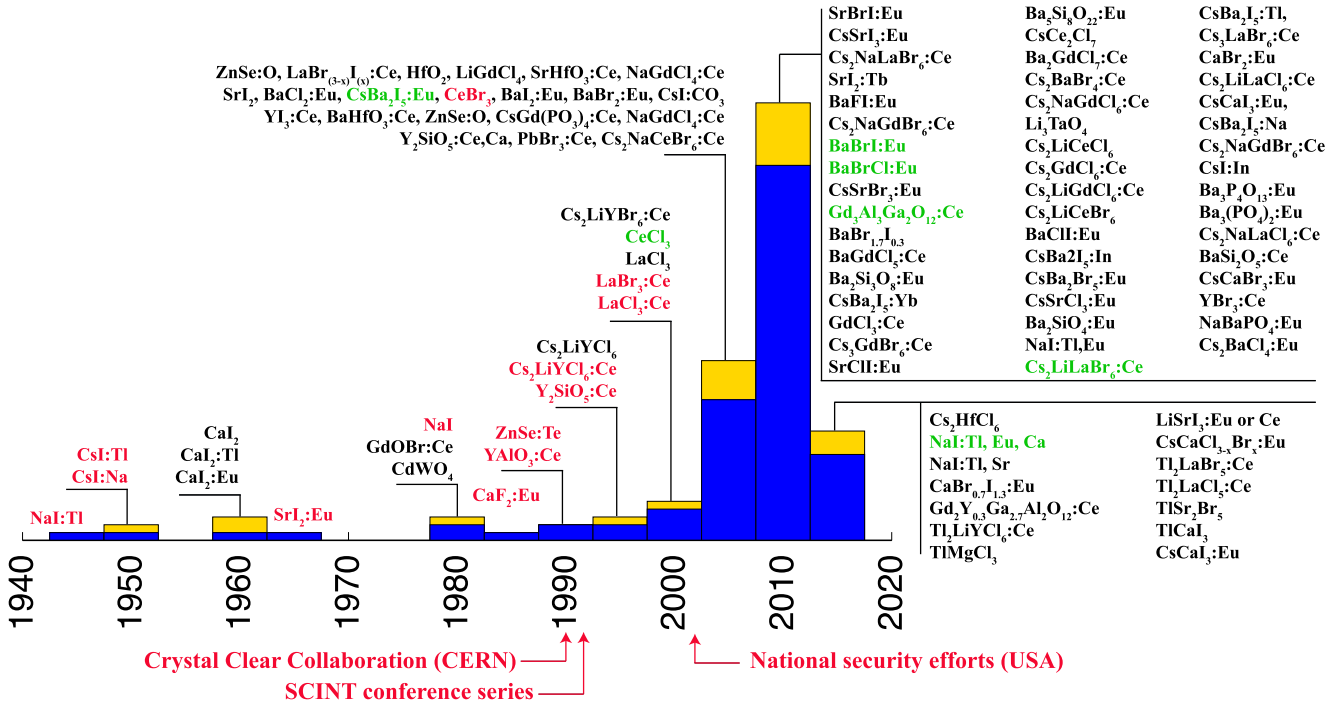

Fig. 1. History (1940–2017) of first publication of scintillators with light output of >20 000 ph/MeV, representing scintillators published in peer-reviewed articles, excluding those containing Rb, Lu, and K due to a high natural radioactivity background not suited for the national security applications. Blue bars: new compounds. Yellow bars: known compounds with new activator or codoped. Red letters: commercial products. Green letters: under development.

- *Improved Understanding of Scintillation Physics:* Development and implementation of dedicated experimental tools and use of advanced computation approaches.
- *Modern Approach to Process Development:* Simulation and modeling of single-crystal growth and visualization/*in situ* diagnostics tools.

The discovery of beneficial defect such as those introduced by codoping (see the following) has opened possibilities to improve some characteristics of a scintillator. Most notable is the improvement of the classic NaI:Tl scintillator used in many national security applications: improvement of its light output [10], energy resolution [11], and of both light output and energy resolution [12]. Consequently, improvements in key characteristics through materials engineering can dramatically improve capabilities and, in some cases, enable new capabilities. While better radiation detector materials can have significant benefit to both passive and active detection systems, it is now recognized that different applications will have different detector requirements. From progress in understanding the scintillation mechanisms, we are now in a position to better infer how to tailor the properties of a scintillator for specific nuclear detection applications.

B. Fast Timing

If the search and development of scintillators has been for a long time mainly focusing on improving the light yield and energy proportionality response in order to improve the energy resolution, a new trend for fast timing capability has recently emerged. This new requirement is mainly driven by HEP experiments to cope with higher event rates while minimizing pileup at high-luminosity colliders, as well as by TOF-PET applications to improve the image signal-to-noise ratio (SNR), with a first application for overweight patients and, ultimately, for opening the way to reconstructionless PET imaging. Timing resolutions in the 10-ps range are required in both cases, which boosts the research for scintillators with a high light yield, a short rise time, and a decay time, as well as for ultrafast scintillation mechanisms to produce prompt photons as a result of transient phenomena and/or quantum confinement.

1) Requirements for Particle Physics Experiments: In the search for rare events, high-luminosity hadron colliders operate at high collision rates, which requires a short time response of the detectors. Decay times of the order of the bunch crossing time (25 ns at Large Hadron Collider (LHC), but as short at 500 ps for the compact linear collider [13]), are necessary. The correct identification of bunches at the origin of an event implies, therefore, a timing resolution of at least 500 ps for all the recorded by-products of this event (particle tracks or energy deposited in calorimeters). Moreover, the high track density and event pileup pose serious challenges for physics event reconstruction and analysis. For energy measurements, one important source of degradation is represented by the contamination of neutral particles originating from secondary vertexes. A precise timing of both calorimeter deposits and vertexes can aid in the reconstruction, allowing the rejection of spurious energy deposits that are not consistent with the primary vertex time. At LHC, CERN, up to 40 pileup events can be produced at each bunch crossing at the designed luminosity of 2×10^{34} cm^{-2}s^{-1}, which will

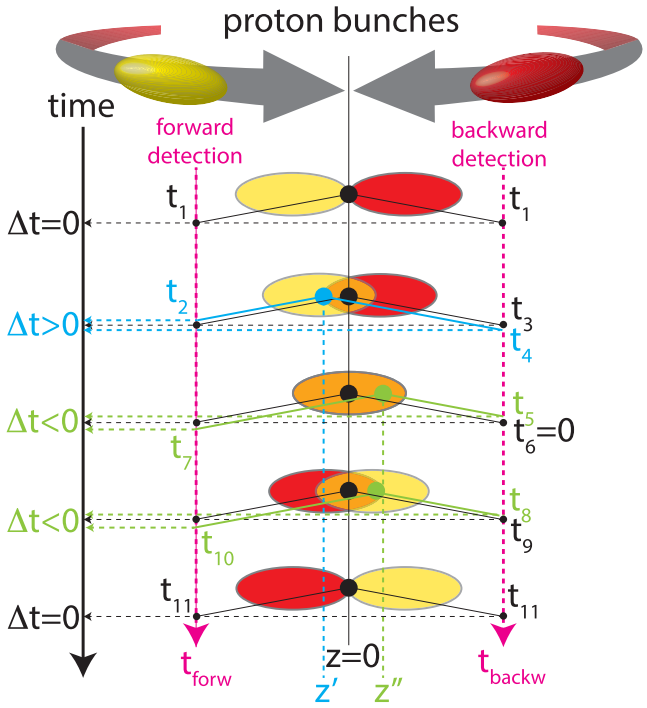

Fig. 2. Schematics of bunch crossing and TOF in the forward and backward directions of particles generated by the events created in different positions of the overlap region.

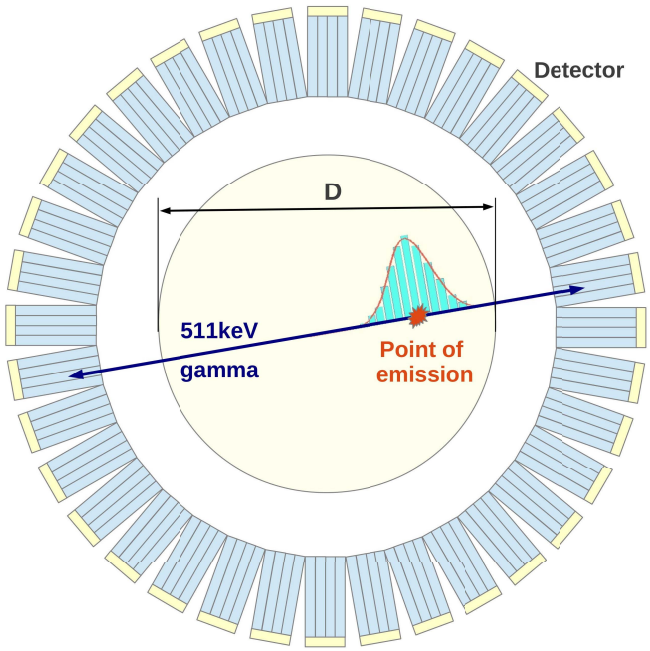

Fig. 3. TOF information in PET constraints the positron emission region along the LOR, leading to an improved SNR.

reach 200 pileup events when the luminosity will be increased to 10^{35} cm^{-2}s^{-1} at the high-luminosity LHC [14]. For a luminosity region of about 10 cm (bunch length), the collisions will be distributed over 300 ps (see Fig. 2). Precise association of collision tracks or jets would help mitigate the pileup. If this can be done for charged particles at high transverse momentum with particle tracking detectors, this approach will be much more difficult in the forward–backward region and even impossible for neutral particles. In this case, only TOF techniques can be applied as shown in Fig. 2 (right), where the two crossing bunches are symbolized by gray and red bunches and the overlapping area is represented by a combination of those colors. Events generated in the middle of the experiment ($z = 0$) will generate tracks arriving at the same time in the forward and backward regions. On the other hand, events generated at any time off-center of the bunch-overlapping region will exhibit a TOF difference for the tracks generated in the forward and backward regions, as shown in Fig. 2 (t_2–t_4 and t_5–t_7). A mitigation factor of one order of magnitude necessitates a TOF precision of at least 30 ps [14].

2) Requirements for Medical Imaging: In the domain of medical imaging, a new generation of TOF-PET scanners offers significant improvements in image quality. In a PET system, the image quality determined by the SNR can be drastically improved by using TOF information [15]. This additional time information improves the prior information on the exact localization of the positron emission point in the line of response (LOR) and, thus, contributes to the rejection of background events outside the region of interest, reducing the noise in the reconstructed image and increasing the image contrast. Without any time information, all points along the LOR have the same probability of being the origin of the β^+ emission, i.e., being emitted by the cancer cells, as shown in Fig. 3. Including the TOF information, a certain region of the LOR can be identified to have the highest probability of being the origin of the β^+ emission. The image SNR gain of a TOF-PET system compared to a non-TOF-PET system can be expressed by the following equation, as described in [16]:

$$G = \frac{\mathrm{SNR_{TOF}}}{\mathrm{SNR_{non-TOF}}} = \sqrt{\frac{2D}{c \cdot \mathrm{CTR}}} \tag{1}$$

where D denotes the diameter of the volume to be examined (the patient dimensions), c is the speed of light in vacuum, and CTR is the coincidence time resolution achieved by the system. Assuming a patient diameter D of 40 cm (D = 40 cm), the SNR gain can reach a factor of 2.3, 5.2, and 16.4 for a CTR resolution of 500, 100, and 10 ps, respectively.

Until recently, PET scanners did not have any TOF capability to localize the position of the positron decay along the LOR of the two γ-rays. Developments in fast scintillation crystals, photodetectors, and electronics have opened the way to TOF-PET scanners with CTR, improving progressively from 500–600 to 249 ps as recently announced by Siemens for their Biograph Vision scanner. Breaking significantly, the 100-ps barrier would not only dramatically improve the SNR, but the possibility to significantly remove artifacts affecting tomographic reconstruction in the case of partial angular coverage will open the field to a larger variety of organ-specific imaging device as well as to imaging-assisted minimally invasive interventions by endoscopy. Ultimately, a time resolution of 10 ps would lead to an uncertainty of only 1.5 mm for a given positron disintegration along the corresponding LOR. Such accuracy is of the order of today's very best small animal or organ-specific PET spatial resolution. The time-consuming tomographic backprojection or iterative

reconstruction algorithms would be considerably reduced, as true 3-D information would be directly available for each decay event [17]. The possibility to see in real time, the accumulation of the events during the acquisition could introduce a paradigm shift in routine clinical protocols, allowing in particular to adapt the acquisition time to what is really observed and not to some predetermined evaluation. Moreover, such a timing resolution would allow recording the full sequence of all γ-ray interactions inside the scanner, including Compton interactions, such as in a 3-D movie, opening the way to the integration of at least a fraction of the Compton events in the image reconstruction and to a further improvement in sensitivity. Hadron therapy would also greatly benefit from a fast online monitoring of the dose delivered during proton or carbon therapy treatment, requiring very high sensitivity, high resolution, and fast reconstruction imaging of β^+-emitting isotopes produced by beam or target spallation processes during the irradiation [18].

3) Requirements for Safety Systems and Homeland Security: Scintillators are used in three main types of equipment related to safety and homeland security: express control of luggage and passengers, search for explosive materials, and remote detection of fissile materials. Luggage inspection requires the highest possible throughput to quickly identify a suspect luggage in a few cubic meter large container moving across the inspection device. The spatial resolution is determined by the need to quickly localize and identify the suspect object in a large container. Fast scintillation kinetics with no afterglow is therefore the most important parameter. For the remote detection of explosives, the most attractive methods are based on the detection of natural or induced characteristic neutron and γ-rays under activation by a neutron source, either with fast neutrons from the ^{252}Cf radioisotope or fast-thermal neutrons from a pulsed electronic neutron generator. For such applications, fast scintillation decay time is important to allow TOF analysis with pulsed neutron generators and more generally for the detection of fast neutrons. Finally, there is an increasing demand for ultrafast X-ray imaging systems to visualize the dynamic behavior of transient phenomena in a dusty environment, such as the impact of projectiles on some targets.

4) Possible Avenues for the Development of Ultrafast Scintillators: Achieving ultimate time resolution on scintillator-based detectors requires a parallel effort on the light production mechanisms, light transport optimization to reduce the travel time spread of the photons on their way to the photodetector, on the photoconversion system, as well as on the readout electronics. The time resolution of a scintillator-based detector is directly driven by the density of photoelectrons generated in the photodetector at the leading edge of the signal. Increasing the light output, and, as a consequence, the rate of photoelectrons produced in the photodetector at the early stage of the signal generation, has a direct impact on the timing resolution by the virtue of the improved photostatistics as illustrated by the following formula derived from Hyman theory:

$$\Delta t \propto \frac{\sqrt{\tau}}{\sqrt{N_{\text{phe}}/\text{ENF}}} \tag{2}$$

where τ is the scintillator decay time, N_{phe} is the number of photoelectrons, and ENF is the excess noise factor of the photodetector. Only optically allowed (interconfiguration) transitions (such as the transition $5d \rightarrow 4f$ for Ce^{3+}), cross luminescence, which is intrinsically fast and temperature independent as observed in barium fluoride (BaF_2), and strongly quenched intrinsic luminescence (as for $PbWO_4$ (PWO)) can give rise to a fast light signal. Besides the gain in photostatistics, another factor, not apparent in this simplified formula, plays a determinant role for the timing resolution. It is related to the scintillator rise time that affects the photoelectron density in the early stage of the signal, which carries the ultimate timing information [19], [20] transition on the activator ion or on the intrinsic luminescent center, only takes place after a complex relaxation mechanism of the primary electron–hole pairs that can last several nanoseconds. In this process, large statistical fluctuations are therefore induced for the generation of the first scintillation photons that influence the observed rise time. This presents an intrinsic limit to the achievable time resolution in a scintillator. It is related to the time fluctuations in the relaxation process that can be estimated to be of the order of 100 ps. For sub-100-ps time resolution, mechanisms involving the production of prompt photons need to be considered. Cerenkov emission and cross luminescent materials can offer a solution. However, the number of Cerenkov photons from the recoil electrons resulting from a 511-keV γ conversion is very small, of the order of 20 photons in crystals, such as Lu_2SiO_5:Ce^{3+} (LSO), $LuAlO_3$:Ce^{3+}, and Gd_2SiO_5:Ce^{3+}. Moreover, these photons are preferentially emitted in the UV part of the spectrum, where the optical transmittance and the photodetector quantum efficiency are generally low. The same applies for cross luminescent materials characterized by a reasonably fast emission (600 ps for BaF_2) which emit in a spectral range of about 250 nm. However, some transient phenomena in the relaxation process can be possibly exploited for the generation of prompt photons. From this point of view, an interesting phase of the relaxation mechanism is the thermalization step when the hot electrons and holes have passed the ionization threshold. The coupling to acoustic and optical phonons in the lattice is the source of hot intraband luminescence (HIBL) that could be exploited to obtain a time tag for the interaction of ionizing radiation with a precision in the picosecond range [21]. This emission is rather weak but extremely fast (sub-ps), and it is characterized by a flat spectrum in the visible for the electron-induced HIBL in the conduction band with an onset in the near infrared attributed to the hole HIBL in the valence band. A few hundreds of prompt photons would suffice to significantly improve the time resolution of scintillators, such as LSO in the low energy (MeV) regime. A novel route toward the realization of ultrafast timing resolution is possible with the use of heterostructures based on a combination of standard scintillators (such as LSO or LYSO), and nanocrystals could be another way to produce prompt photons. Nanocrystals have gained considerable attention over the last two decades because of their excellent fluorescence properties. In such systems, the quantum confinement offers very attractive properties, such as a very high quantum efficiency and ultrafast decay time. Moreover, they

TABLE I
REQUIREMENTS ON HARD X-RAY IMAGERS FOR THE PROPOSED MARIE PROJECT

Performance	Type I imager	Type II imager
X-ray energy	up to 30 keV	42-126 keV
Frame-rate/inter-frame time	0.5 GHz/2 ns	3 GHz/300 ps
Number of frames per burst	10	10 - 30
X-ray detection efficiency	above 50%	above 80%
Pixel size/pitch	$\leqslant$300 μm	$<$300 μm
Dynamic range	10^3 X-ph./pix./fr.	$\geqslant 10^4$ X-ph./pix./fr.
Pixel format	64 x 64	1 Mpix

have a broadband absorption, narrow emission, and enhanced stability compared to organic dyes, and the fluorescence is tunable from the UV to the near-infrared spectral range (300–3000 nm) by nanocrystal size and material composition.

C. Fast Imaging

As discussed previously, the ultrafast hard X-ray imaging is an emerging need. Substantial advances have been made in high-speed imaging technologies, including ones for the full spectrum of X-ray wavelengths. Dedicated high-speed imaging technologies have been developed for the existing and upcoming X-ray free electron lasers (XFELs), such as LCLS, European XFEL, SACLA, and SwissFEL. Commercial photon-counting cameras, such as Pilatus, X-ray integrating detectors or high-speed visible light charge coupled device, and CMOS cameras in conjunction with fast scintillators, are used for many experiments when dedicated imaging technologies are not available. State-of-the-art X-ray imaging cameras use silicon sensors for X-ray detection and have demonstrated a frame rate close to 10 MHz and excellent performance for X-ray imaging at energies below 20 keV. Prototype high frame rate imaging cameras with high atomic weight sensors have recently been demonstrated.

Aiming at studying the dynamics of material evolution related to the nuclear Big Bang, the Matter–Radiation Interaction in Extreme (MaRIE) facility was proposed at the Los Alamos National Laboratory [22], where GHz hard X-ray ($>$20 keV) imaging is required. Table I summarizes the requirements on hard X-ray imagers for the proposed MaRIE project [23], where 2-ns and 300-ps frame rates are required for the type I and type II imagers, respectively, for X-rays up to 30 and 126 keV. To mitigate the pileup effect for such fast frame rate, it is important to have a temporal response of the X-ray signals of less than 2 ns and 300 ps, respectively, for the Types I and II imagers. The development of sensors with ultrafast response for such imager, thus, is important.

Two types of sensor technologies are being pursued for fast X-ray imaging [23]. The direct sensor technology uses semiconductor devices to convert X-rays to electrons and to collect them. The indirect sensor technology uses inorganic scintillators to convert X-rays to photons collected by photodetectors. Both direct and indirect sensors for X-ray detection are currently limited by the materials and their structures. There is a significant gap between the state-of-the-art X-ray imaging technologies at about 10-MHz frame rate and the desired performances for the proposed MaRIE project. While the direct technology prevails in MHz soft X-ray imaging, it has an intrinsic limitation for the GHz hard X-ray imaging because of the low detection efficiency of thin detectors required for fast response. Development of ultrafast inorganic scintillators with fast rising time, fast decay time, and negligible slow scintillation tail, thus, is crucial for such imagers.

In the past three years, investigations have been carried out to identify ultrafast inorganic crystal scintillators for the GHz hard X-ray imaging [24], [25]. Among them, cerium-doped or Ce/Ca-codoped lutetium oxyorthosilicate (LSO:Ce) and lutetium yttrium oxyorthosilicate (LYSO:Ce) are known for their superb performances and wide applications, but they are too slow for that application. While $LaBr_3$:Ce and $CeBr_3$ are brighter and faster than LYSO:Ce, they are, as well, still not fast enough because of their decay time of longer than 10 ns, which would cause significant pileup at the GHz scale. Among all crystals, known scintillators, only two (BaF_2 and ZnO and its analog doped with Ga), show ultrafast scintillation light with sub-ns decay time required for the GHz hard X-ray imaging, but both materials have relatively lower overall light output as compared to LYSO:Ce. Their light output in the first ns, however, is compatible with LYSO:Ce because of their sub-ns decay time. BaF_2 is also featured with the shortest attenuation length for 40-keV X-rays, promising a compact sensor for the GHz hard X-ray imaging. The real issues for these materials are the slow component for BaF_2 with 600-ns decay time, which would cause pileup and the self-absorption for ZnO that prevents its use in bulk. Progresses were reported in the SCINT 2017 conference at Chamonix, France, in both materials. Yttrium doping in BaF_2 is found to be effective in improving the fast/slow ratio from 1/5 to 6/1 while keeping the amount of the fast scintillation component with sub-ns FWHM width unchanged [26]. ZnO nanoparticles embedded in polystyrene show a 0.5-ns decay time [27].

Two inorganic scintillator-based imager concepts were reported in the SCINT 2017 conference. Fig. 4 (top) shows a total absorption X-ray imager, where pixelated BaF_2 crystals are coupled to a matching pixelated photodetector and readout by fast electronics [23]. This approach is similar to an ultrafast BaF_2 crystal calorimeter being pursued by the HEP community [28]. A joint development program with the HEP community, thus, will benefit both fields. Another approach is to use thin layer films coated with ZnO:Ga nanoparticles. Fig. 4 (bottom) shows an imager featured with multilayer high quantum efficiency photocathode coated with ZnO:Ga nanoparticles [24].

While research and development continues to develop these detector concepts, development of ultrafast inorganic crystal scintillators is expected to play a crucial role for the GHz hard X-ray imaging. For the type II imager, for example, a decay time of less than 300 ps is required.

D. Fast Neutron Detection

^{3}He has been the standard for neutron detection and it is widely believed that its performance cannot be surpassed, especially its excellent neutron detection and gamma-ray rejection. However, direct detection of fast neutrons is not

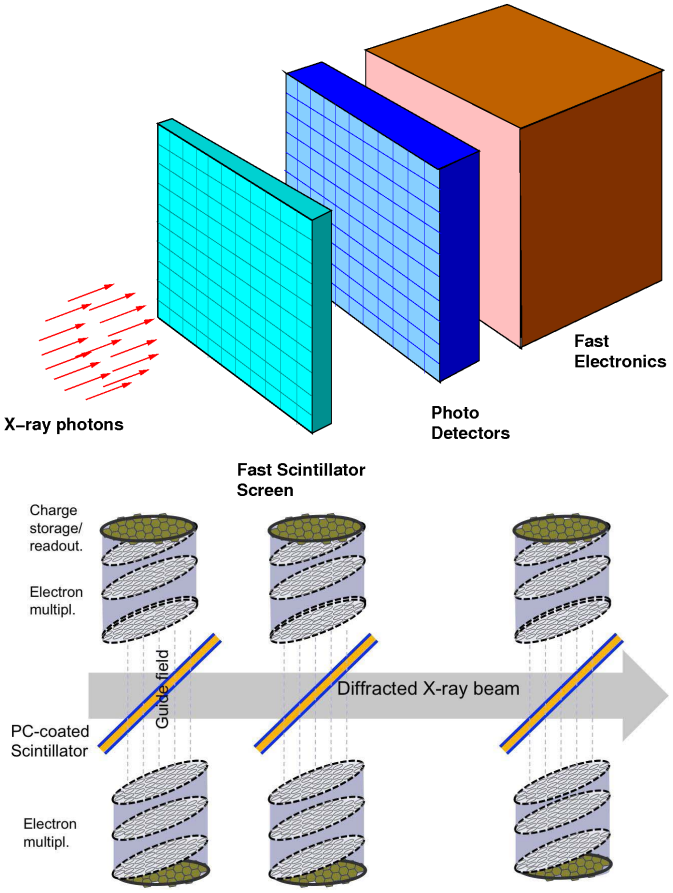

Fig. 4. Top: pixelated total absorption imager. Bottom: multilayer thin film imager.

possible and a moderator is used to slow down the high-energy neutrons. Fast neutrons are the signature of plutonium, and the localization of sources is critical for nuclear plant safety and decommissioning as well as for detection of illicit transport of nuclear materials. Inorganic scintillators are currently absent from development efforts for detection of fast neutron as H is the element of choice most easily found in organic compounds and plastics are currently dominating the research efforts. The organic crystal stilbene is being tested due to its good neutron–gamma discrimination but its fragile nature and the relatively large volume needed for the applications may restrict its use. Recently, an organic glass was developed that exceeds the performance of stilbene in both luminosity and neutron–gamma discrimination [29]. With the development of inorganic scintillators in other form than large single crystals, such as fibers, transparent ceramics, nanosize particles, and so on, it is likely that organic–inorganic composite materials could be developed making complete separation of gamma and neutron detection possible or more generally separating specific functionalities of the phases in a multicomponent material.

E. High Energy Calorimetry

In HEP and nuclear physics experiments, total absorption electromagnetic calorimeters made of inorganic crystals are known for their superb energy resolution and detection efficiency for photon and electron measurements. An inorganic crystal calorimeter is, thus, the choice for those experiments where precision measurements of photons and electrons are crucial for their physics missions. Examples are the crystal ball NaI:Tl calorimeter, the L3 BGO calorimeter, the BaBar CsI:Tl calorimeter, the BELLE CsI:Tl calorimeter and the BES-II CsI:Tl calorimeter in lepton colliders, the kTeV-undoped CsI calorimeter and the compact muon solenoid (CMS) PWO calorimeter in hadron colliders, and the Fermi CsI:Tl calorimeter, the DAMPE BGO calorimeter, and the HDME LYSO calorimeter in space. Table II lists design parameters for some crystal calorimeters built for HEP experiments since the 1970s [30]. Among all existing crystal calorimeters, the CMS lead tungstate ($PbWO_4$ or PWO) crystal calorimeter, consisting of 75 848 crystals of 11 m^3, is the largest. Because of its superb energy resolution and detection efficiency, the CMS PWO calorimeter has played an important role for the discovery of the Higgs boson by the CMS experiment [31]. Crystal calorimeters currently under construction are an undoped CsI calorimeter for the Mu2e experiment at Fermilab, a PWO calorimeter for PANDA at the Facility for Antiproton and Ion Research, a LYSO calorimeter for COMET at J-PARC and a PbF_2 calorimeter for the g-2 experiment at Fermilab. Future HEP calorimeters will be operated under unprecedented luminosity. A crucial issue is, thus, the decay time of the scintillation light. In [30], there are listed the optical and scintillation properties for fast inorganic crystal scintillators with a scintillation decay time ranging from subnanosecond to a few tens of nanoseconds, and compared with plastic scintillator. Among the fast crystals, the mass production cost of barium fluoride (BaF_2) and undoped CsI crystals is significantly lower than others because of their low raw material cost and low melting point. Crystal calorimeters for future HEP experiments at the energy frontier face the challenge of severe radiation environment. Significant loss of light output has been observed in the CMS PWO crystals at large rapidity *in situ* at the LHC caused by both ionization dose and hadrons [32]. Significant contributions in improving radiation hardness of inorganic crystal scintillators have been achieved. Controlling oxygen contamination in halide crystals, e.g., CsI:Tl, or oxygen vacancies in oxide crystals, e.g., PWO, was found effective [33]. Codoping with yttrium and lanthanum was also found effective for CMS PWO crystals [34]. For experiments to be operated at the high luminosity LHC (HL-LHC) with 3000 fb^{-1}, crystals should survive an environment with an absorbed dose of 100 Mrad, charged hadron fluence of 6 10^{14} cm^{-2} and fast neutron fluence of 3 10^{15} cm^{-2}. To mitigate this challenge, efforts have been made to reduce the light path length in the crystals by designing an inorganic scintillator-based shashlik sampling calorimeter [35]. On the other hand, investigations of radiation hardness of inorganic scintillators to such a level have also been carried out. Radiation damage in various inorganic crystal scintillators has been investigated for an ionization dose up to 340 Mrad [36]–[38] and a fluence of protons up to 3×10^{15} cm^{-2} [39]. Progress on neutron-induced radiation damage up to 3×10^{15} cm^{-2} was also reported in the SCINT 2017 conference [40]. BaF_2-, GAGG-, LuAG-, and LYSO-based inorganic scintillators are found to be radiation hard for the HL-LHC. Following these investigations, a LYSO MIP

TABLE II
EXISTING CRYSTAL CALORIMETERS IN HEP

Date	**75-85**	**80-00**	**80-00**	**80-00**	**90-10**	**94-10**	**94-10**	**95-20**
Experiment	C.Ball	L3	CLEO II	C.Barrel	kTeV	BaBar	BELLE	CMS
Accelerator	SPEAR	LEP	CESR	LEAR	Tevatron	PEP	KEKB	LHC
Laboratory	SLAC	CERN	Cornell	CERN	FNAL	SLAC	KEK	CERN
Crystal Type	NaI:Tl	BGO	CsI:Tl	CsI:Tl	CsI	CsI:Tl	CsI:Tl	PWO
B-Field (T)	-	0.5	1.5	1.5	-	1.5	1.0	4.0
r_{inner} (m)	0.254	0.55	1.0	0.27	-	1.0	1.25	1.29
Crystal number	672	11,400	7,800	1,400	3,300	6,580	8,800	75,848
Crystal DepthX0	16	22	16	16	27	16 to 17.5	16.2	25
Crystal Volumem^3	1	1.5	7	1	2	5.9	9.5	11
Light Outputp.e./MeV	350	1,400	5,000	2,000	40	5,000	5,000	2
Photo-detector	PMT	Si PD	Si PD	WS+Si PD	PMT	Si PD	Si PD	Si APD
Gain of Photo-detector	Large	1	1	1	4,000	1	1	50
σ_N/ChannelMeV	0.05	0.8	0.5	0.2	Small	0.15	0.2	40
Dynamic Range	10^4	10^5	10^4	10^4	10^4	10^4	10^4	10^5

timing detector has been proposed for the CMS upgrade for the HL-LHC [41].

Another challenge for future HEP experiments at the intensity frontier, such as Mu2e-II, is the unprecedented event rate at a level of about 10 ns [42]. Such a fast rate requires ultrafast scintillators to mitigate the effect of pileup. Research and development aimed at developing ultrafast inorganic scintillators has also been pursued by the SCINT community, and the progress was reported in the SCINT 2017 conference. Yttrium doping in BaF_2 crystals was found to be effective to suppress the slow scintillation component in BaF_2 while maintaining the sub-ns fast component [43]. An interesting direction along this direction is to combine confined excitons and biexcitons into a form of nanocrystals in bulk scintillators [44]. For HEP experiments at future lepton colliders, inorganic scintillators have been proposed to build a homogeneous hadron calorimeter (HHCAL) to achieve unprecedented jet mass resolution by dual readout of both Cherenkov and scintillation light [45], [46]. For this application, development of cost-effective crystal detectors is a crucial issue because of the huge crystal volume required, whereas the requirement on radiation hardness is much relaxed because of the lepton collider environment [47]. Investigation along this line has been concentrated on developing cost-effective UV transparent inorganic scintillators, including crystals and glasses. Progress on UV transparent cerium-doped and codoped fluorophosphate glasses was reported at the SCINT 2017 conference [48] and at the NSS 2017 conference [49].

Briefly summarizing, inorganic crystal scintillators have played an important role in HEP experiments in the past, and new generations of scintillators are expected to play an important one as well. The main challenge in this application is to develop ultrafast and radiation hard inorganic scintillators for future HEP experiments at the energy and intensity frontiers. Additional challenges are to develop UV-transparent cost-effective inorganic scintillators for the HHCAL detector concept. Successful development along these lines of research is also expected to benefit GHz hard X-ray imaging being pursued by the nuclear physics community and for medical imaging.

F. Scintillation Pulse Detection

With analog pulse shape techniques, the integral intensity of a pulse is digitized that provides pulse height spectra from which the energy resolution and scintillation light yield can be determined. The pulse shape can be recorded with start–stop methods from which the scintillation decay time components can be determined. Waveform digitizing where each scintillation pulse is stored individually and analyzed off-line is an emerging technology that is bound to replace the traditional techniques. It requires a waveform digitizer, electronic storage capacity, and software to study, analyze, and sort each stored scintillation pulse. Applications for particle discrimination based on online pulse shape analysis are fairly obvious [50], [51]. However, when the photon detector output from a scintillator is fully digitized, then for each pulse, the intensity as function of time is available, and we have full information of our scintillator. The potential of the methods was presented in recent contributions [52], [53]. By offline integration of the pulses, a pulse height spectrum can be generated. One may also sort the pulses of similar pulse height and study the pulse shape as a function of pulse height. The energy dependence of scintillation decay time components can then be derived. Such found dependence was exploited to improve energy resolution, and discrimination of α and γ events was demonstrated [52], [53]. Digitization was applied to determine the contribution of alpha decay of intrinsic radioactive isotopes present in La halide scintillators. Scintillation pulses from the parent and daughter nuclei could be traced by a search for time correlated scintillation events. One may then discriminate different alpha decays in the intrinsic pulse height spectrum of La halides. The emerging digitizing techniques may lead to different research strategies for finding better scintillation materials. If both scintillation pulse height and pulse shape depend on gamma photon energy, then knowing both, the gamma energy can be determined more accurately. One may then search for scintillators with strong shape energy dependence.

III. MATERIAL COMPOSITION

A. Single Crystals

Single crystals are still the dominant bulk form for inorganic scintillator materials. However, the limitations that are imposed by the production process have enticed researchers to look for and develop alternate media, such as transparent ceramics, especially for applications that require very large volume or areas, and composite materials in attempt to couple

specific functions of the different phases. In this section, we discuss recent developments and trends in inorganic scintillator grown as single crystals and produced as transparent ceramics. Eutectics as an example of composite materials are discussed in Section IV. In general, oxides crystals are grown by the Czochralski technique [54] that is a favorite for large scale production. The technique can be fully automated, the growth of the crystal is controlled in real time, and the production yield is high. Iridium crucibles are commonly used for the high melting point oxides that limit the use of oxygen in growth atmosphere to a very low percentage.

Many studies aimed at the optimization of yttrium aluminum garnet YAG: Ce have resulted in an optimized garnet by the substitution of Gd for Y and by alloying of Al with Ga [55]–[57]. The presence of gallium oxide complicates somewhat the growth process as low level of oxygen must be used to prevent its decomposition. However, the growth of single crystals of the Ce-doped garnet $Gd_3Al_2Ga_3O_{12}$, 3 inch diameter has been reported [58] [see Fig. 5(a)] as well as that of 2 inch diameter single crystals of codoped versions of the same composition [59]–[61]. These Ce-doped garnets are now commercially available [62], and the use of codopants allows to tailor one or more characteristics: for example, timing and light output or energy resolution (see Section III-C).

Concerning the halides, scale-up efforts have continued for the binary compound SrI_2:Eu, now available commercially. As the material is deliquescent, proper handling and quality of raw materials have been studied [63]. Most efforts are done using the Bridgman technique with the following two notable exceptions.

- The growth of that material has been demonstrated by the Czochralski technique [64] for diameter up to 50 mm [see Fig. 5(b)].
- A new growth technique similar to a seeded vertical Bridgman technique that uses a graphite crucible in an evacuated dry chamber [55], [65], which allows production at high yield [see Fig. 5(c)].

Even though NaI:Tl and $LaBr_3$:Ce are grown by the Czochralski technique in production plant, the newly discovered multicomponent halide scintillators are mainly grown by the modified Bridgman–Stockbarger techniques due to their reactivity and hygroscopicity that require the materials to be grown in chemically compatible crucibles and dry atmosphere. The Bridgman–Stockbarger technique is easy to implement in a research laboratory as its simplicity implies low starting costs. However, the technique has in general a low yield, especially when used without a seed which is done for the majority of research efforts. Confinement in a crucible (usually quartz that can be sealed easily) or vitreous carbon inserted in a quartz ampoule can induce contamination, sticking of the crystal to the ampoule, and cracking. The lack of reproducibility and low yield is well documented and can be spotted in many publications as, for example, in attempts to grow several crystals in one furnace [66]. As a result, scale-up efforts are still limited for these newly discovered scintillators. Most new multicomponent materials are grown in size less than 25 mm in diameter. We must note that a few attempts at growing these compounds by the Czochralski technique have demonstrated that it is viable and should be pursued [67].

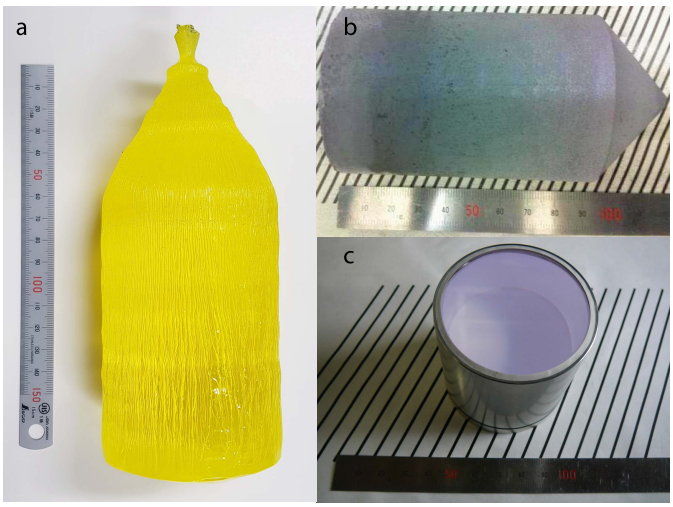

Fig. 5. (a) 3-inch diameter Ce:GAGG crystal grown by the Czochralski method. (b) 2-inch SrI_2:Eu^{2+}. (c) Sealed 2-inch SrI_2:Eu^{2+}. Courtesy of C&A Corporation for all the pictures.

B. Transparent Ceramics

Transparent ceramics are often seen as an alternative to single crystals when a specific geometrical form is not easily achieved with single crystals and in cases where they are produced at a lower cost. However, transparency implies lack of light scattering that can be caused by small defects, such as micropores or disturbances at grain boundaries. Birefringence can also cause scattering when it occurs in noncubic materials and must be control by judicious grain size [68]. In a book published in 2013, Nikl *et al.* [69] noted "the most studied group of materials are the cubic structure aluminum or multicomponent garnets, but interesting results have been achieved also in sesquioxide, silicate, hafnate, complex perovskite, or rare earth halide compounds." This statement still holds today. However, in the last few years, there has been a significant shift in the ceramic studies of the multicomponent garnets in moving from process optimization to performance optimization. Some of the findings from single crystals work are being applied to transparent ceramics: for example, codoping for removal of afterglow or slow decay components [43]. Powder preparation prior to sintering is critical and has been extensively studied with major progress in control of particle size and distribution that is a direct consequence of the development of nanopowders, now commercially available for a large variety of compounds. A successful example of improvement transparent GYGAG ceramic is shown in [70] [see Fig. 6(a)]. Transmission of oxide transparent ceramics can still be improved: structural disturbances at grain boundaries were shown in the cubic material LuAG:Ce [71]. Fabrication of transparent ceramics of hygroscopic halide materials is more challenging due to their reactivity, and few results have been published. Attempts were made to produce SrI_2:Eu as a transparent ceramic [72] with limited success. SrI_2 is orthorhombic, and issues of scattering were not resolved.

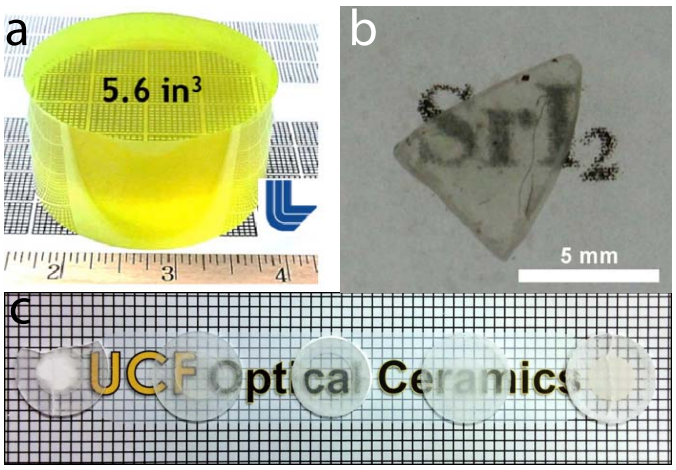

Fig. 6. (a) 5.6-inch^3 GYGAG:Ce transparent ceramic [70]. (b) Translucent ceramic sample of 0.77-mm-thick Eu:SrI backlit [72]. (c) Side-by-side comparison of 1-mm-thick $BaCl_2$ ceramic samples hot pressed at five different temperatures. The $BaCl_2$ core of each sample is surrounded by an outer rim of NaCl [73].

In particular, small grain sizes could not be produced at the chosen sintering conditions [see Fig. 6(b)]. $BaCl_2$:Eu was the topic of a Ph.D. thesis [73]. Powder preparation, an innovative press to control moisture prior to and during sintering, and a high pressure—low-temperature sintering process to limit grain growth are presented in that work [see Fig. 6(c)]. Scintillators of the elpasolite structure are cubic materials that could be made as transparent ceramics if the hurdles linked to their reactivity could be overcome. It is a particularly interesting prospect for those elpasolites that exhibit phase separation in the liquid phase as the sintering could be done in a temperature range that preserves the stable room temperature phase.

C. Codoping

Given the fact that the scintillation mechanism includes a transfer stage in which the migrating electrons and holes in the conduction and valence bands, respectively, must overcome hurdles on their path to reach the emission center, the atomistic perfectness of the scintillator material becomes critical. Even in high-quality single-crystal hosts, there are inevitable point defects, mostly cationic and anionic vacancies, which give rise to hole and electron traps, respectively. Other kinds of lattice disorders, accidental impurities and more extended lattice flaws (e.g., dislocations), can give rise to charge traps as well. Optimization of manufacturing technology cannot completely suppress these defects, and therefore, other tools have been and are being developed to improve scintillator properties dictated by specific applications. One of these tools is the codoping of the scintillator material, the addition of a specific impurity that can (or cannot) participate in charge carrier capture. A well-known example is the codoping of Gd_2O_2S:Pr, phosphor, or ceramic by Ce^{3+} and F^- ions [74], which successfully diminishes the afterglow and enabled its use in computed tomography (CT) medical imaging. Analogously, the Pr-codoping in $(Y,Gd)_2O_3:Eu^{3+}$ ceramics suppresses the afterglow down to 0.005% [75] and enabled its use in the same field. The mechanism of afterglow suppression consists of the nonradiative recombination of charge carriers released from the traps at the codopant limiting their (delayed) radiative recombination at the emission centers themselves. In the case of single crystals, the intensively studied case was the trivalent ion (La, Y, Gd, or Lu) and pentavalent (Nb)-doped $PbWO_4$ scintillator where such a doping considerably improved its radiation hardness (i.e., suppressed charge trapping at deep traps) and enabled its usage in the calorimetric detectors at the LHC, CERN (see review papers [76], [77]). Furthermore, in $CdWO_4$, single-crystal codoping with Li has been adopted [78]; the role of Li was explained as a stabilizing agent of accidental Fe and Mn impurities in 2+ valence state [79], which makes them inactive in the charge trapping process related to the afterglow mechanism. It is, thus, another case in which codoping decreased the afterglow and enabled its use in CT imaging. More recently, codoping with aliovalent, optically inactive ions have been reported to improve scintillator characteristics. For instance, codoping by monovalent alkali metal and divalent alkali earth ions was reported in $LaBr_3$:Ce [80], which resulted in the decrease of nonproportionality and improvement of energy resolution down to 2% at 662 keV in the case of Sr codopant [81]. This is the best result ever reported for an inorganic single-crystal scintillator. The explanation of such an effect is certainly nonintuitive and was proposed as an overall reduction of Auger quenching of free carriers due to increase of the Br vacancy concentration and creation of SrLa V_{Br} complexes [82]. Mutual interactions among charge carriers, defects, and luminescence centers, including creation of excitons and carriers self-trapping, in the first few picoseconds of scintillation mechanism (conversion stage) are under intense study by sophisticated experiments and theoretical calculations due to their influence on scintillator nonproportionality and overall efficiency [83]–[87]. Another single-crystal scintillator, where multiple attempts have been made to improve its characteristics regarding afterglow, is the classical CsI:Tl. Namely, the Eu and Sm [88]–[90] followed by Bi [91], [92] and most recently Yb [93] codopants have been reported. For Eu, Sm, and Bi codopants, the afterglow suppression is accompanied by the decrease of light yield. The CsI:Tl, Yb crystals showed an increase of light yield reaching 90 000 ph/MeV and a decrease of afterglow down to 0.035% at 80 ms, a promising outlook for practical applications in CT or any kind of fast frame imaging. Another widely studied case of aliovalent codoping by optically inactive ions is represented by the Ce-doped oxide-based scintillator materials. Starting with the Ce-doped orthosilicates, the improvement of light yield and time response was reported for Ca-codoped Y_2SiO_5:Ce and Lu_2SiO_5:Ce [94]–[96], but no explanation of its mechanism was provided. The explanation based on the stabilization of Ce^{4+} and its positive role in scintillation mechanism was provided for Me^{2+} (Me = Ca, Mg) codoped LYSO:Ce in 2013 [97] using the optical and photoelectron (X-ray Absorption Near Edge Spectroscopy) spectroscopies. This concept has also been successfully adopted in aluminum and multicomponent garnets. Namely, in LuAG:Ce, the codop-

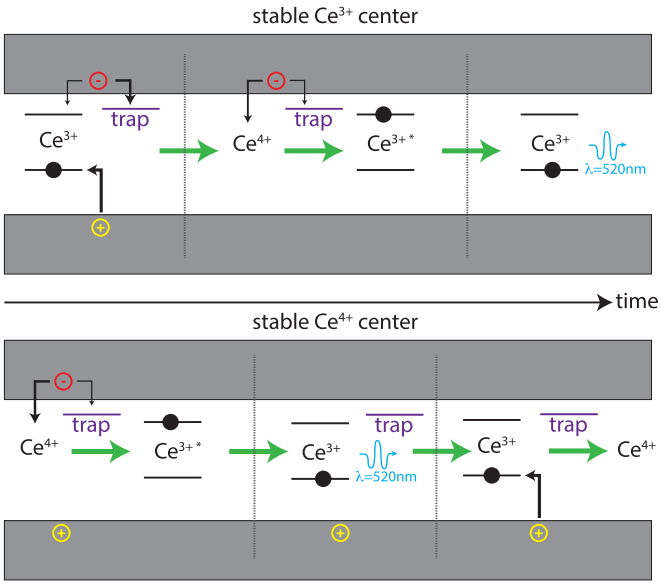

Fig. 7. Sketch of the scintillation mechanism at the stable Ce^{3+} and Ce^{4+} emission centers in an aluminum garnet host. The trap is supposed to be an electron trap. Yellow circle: holes. Red circle: electron. Top gray rectangle: conduction band. Bottom gray rectangle: valence band.

ing by Mg^{2+} both in single crystal [98] and ceramic [99] forms dramatically increased the light yield. For comparable concentration of Mg and Ce in the starting materials used for single-crystal growth when concentration of stable Ce^{4+} prevails over that of Ce^{3+}, the slow scintillation decay components were effectively suppressed. Fig. 7 provides a schematic of the sequences of charge carrier capture at the stable Ce^{3+} and Ce^{4+} emission centers. The Ce^{4+} center can efficiently compete with electron traps of any kind for an immediate capture of electrons from the conduction band, whereas the stable Ce^{3+} center needs first to capture the hole, i.e., much less effective in this competition. As a direct consequence, the presence of stable Ce^{4+} diminishes the amount of delayed light (slow components) in scintillation response that arises from electron trapping. It is worth mentioning that, for both Ce^{3+} and Ce^{4+}, the emission transition is the same, i.e., the produced scintillation spectrum is the same, and that in the last step of the Ce^{4+} scintillation mechanism (right part), the hole capture from the valence band is always nonradiative, i.e., not contributing to afterglow.

In the newly developed single crystals of multicomponent garnets, so-called GAGG:Ce scintillator (host composition within $Gd_3Al_2Ga_3O_{12}$ and $Gd_3Al_3Ga_2O_{12}$) became a material system of interest due to very high light yield approaching 60 000 ph/MeV (see review in [100]). Codoping of GAGG:Ce by divalent Ca and Mg ions always resulted in gradual light yield decrease, Mg^{2+} resulting in a lesser effect [101]. However, this codoping significantly reduced the rise time in its scintillation response and improved its timing coincidence resolution to become comparable with that of LSO:Ce, Ca [37], [60], [102]. This paves the way for its use in TOF techniques, e.g., in TOF-PET medical imaging. This optimization strategy can be efficiently applied only in the absence of overlap between the charge transfer absorption of Ce^{4+} with the onset at about 350–370 nm in an oxide host and the emission of Ce^{3+}. For example, the aluminum perovskite $YAlO_3$:Ce scintillator that emits at 360 nm, Mg^{2+} codoping cannot be used because of large light yield loss, even if the scintillation response is accelerated on the rise time, the fall time, and the slow component, similarly as in aluminum garnets [103]. For the same reason, it cannot be used at all for the Pr^{3+}-doped oxides [104]. From the above-mentioned examples, it becomes evident that further development can be focused on improvement of specific characteristics (afterglow, light yield, nonproportionality, and scintillation response) through targeted action of the codopant. It can work as a simple nonradiative quenching center (Ce^{3+} in Gd_2O_2S:Pr and Pr^{3+} in $(Y,Gd)_2O_3$:Eu), an aliovalent impurity to destabilize accidental impurities from unwanted charge states (Li in $CdWO_4$), an aliovalent impurity that influences charge carrier interactions in very early stage of scintillation mechanism (Sr^{2+} in $LaBr_3$), or an aliovalent impurity that stabilized the emission center itself in another (favorable) charge state. It is also now clear that the action and effect of codopant are host-specific which means that the concept successful in one host cannot be mechanically transferred to another one. For example, it is worth noting that the same charge misbalance induced by doping a divalent cation at a trivalent site induces completely different response from the material when comparing $LaBr_3$:Ce and LuAG:Ce (no Ce^{4+} stabilization in $LaBr_3$ is observed). Consequently, to apply successfully scintillation material engineering by codoping, one has to understand the bottlenecks in its scintillation mechanism, the mechanism of localization of electrons and holes in the material structure, and the creation of intrinsic color centers. Furthermore, given the fact that the codoping is always focused on the defect engineering, the reported concepts should be validated by several independent laboratories to make sure that the observed effects are stable and reproducible. Finally, technological feasibility to add one or more codopants in a reproducible way in the process of material preparation must be ensured.

D. Nanomaterials

Nanoparticles of direct bandgap semiconductors (Q-dots) have attracted a lot of interest for their luminescence properties in the last decades. The scintillating properties of Q-dots have been first presented in 2006 by Létant and Wang [105]. While optical properties of quantum dots are significantly driven by quantum confinement effects, doped insulator nanoparticles do not show any quantum confinement regarding their optical properties due to the strongly localized character of the emission centers. Nevertheless, surface effects and structural disorders might appear and can affect the luminescence yield [106]. Using nanoparticles as scintillator, thus called nanoscintillator, has several potential interests. Nanoscintillators can be embedded in a matrix to imitate bulk material: organic or glassy host has been used [107]–[110] with YSO, $GdBr_3$, or LaF_3 doped with Ce^{3+} as well as CdTe. However, the active volume fraction is limited and

the achieved energy resolution remains poor. In the case of semiconductor quantum dots, this strategy is even more complex as their small Stokes shift renders the extraction of light difficult, and some strategies using a plastic host loaded with dye molecules have been proposed [111]. Here, a complex energy transfer interplay among the matrix, the dye, and the Q-Dot is proposed to overcome the self-absorption issue. The loaded matrix acts as a kind of wavelength shifter, and a rather weak photopeak is detected. For the use as a bulk material, the main benefit could be to combine an active host with a nanoscintillator of special composition in order to enhance neutron cross section as example. Such approach has been proposed using a liquid scintillator loaded with semiconductor Q-dots for antineutrino measurement [112]. Here, the goal was to take advantage of the presence of ^{113}Cd in the nanoparticles to enhance the neutron capture cross section. ^{106}Cd is also of interest because of its capability for double β^+ decay and double β^- capture. Note that there is no need to have a nanoscintillator to obtain cross-sectional enhancements. As described latter, the spatial extension of the energy deposition being larger than the particle size, passive nanoparticle (nonemitting) can also be used as illustrated with undoped Gd_2O_3 nanoparticle in a polymer [113]. The most promising use of nanoscintillators embedded in matrix is to enhance or add one functionality. Interestingly, nanostructures allow to prepare scintillator material in an unusual form. As an illustration, a scintillating membrane based on nanowires of YAG:Er^{3+} has been proposed for measurement of radioactive fluids [114]. Aside from the detection field, the nanoscintillator can also be used as part of therapeutic agent for photodynamic therapy. The concept, proposed in 2006 [115], is to combine a sensitizer able to generate singlet oxygen under appropriate illumination and a nanoscintillator. As described in Fig. 8, such approach enables to overcome the issue of penetration of light in tissue since nanoscintillators can be activated by penetrating X-ray. However, the complex sequence of energy transfer can give rise to the singlet oxygen generation or not, depending on the wavelength emission and main distances between the emitting center and the photosensitizer [116], [117]. Another limitation is probably the weak energy deposition efficiency in the case of nanostructured and diluted media. As described in [118] using Monte Carlo simulations, a correcting efficiency factor of about 1% has to be applied to the predicted efficiency using the effective medium approach proposed in [119] in order to take into account such nonhomogeneous medium. The real efficiency is thus probably quite weak, suggesting it can be applied only under high radiation doses, such as those received during radiotherapy. Note that radiosensitization probably occurs as well. Despite these limitations, enhancement of radiotherapy effect has been observed on cells [120]. These studies suggest that the system is probably not yet optimized and that other more suitable nanoscintillators should be searched for optimizing performances [121], [122]. As described in Section III-B, the nanoscintillator may also address the needs for fast timing. At least, three approaches can be proposed. First, direct bandgap semiconductors are fast emitters, such as CuI, HgI_2, PbI_2, ZnO:Ga, and CdS:In [123]. They can be prepared as nanoparticles with the appropriate

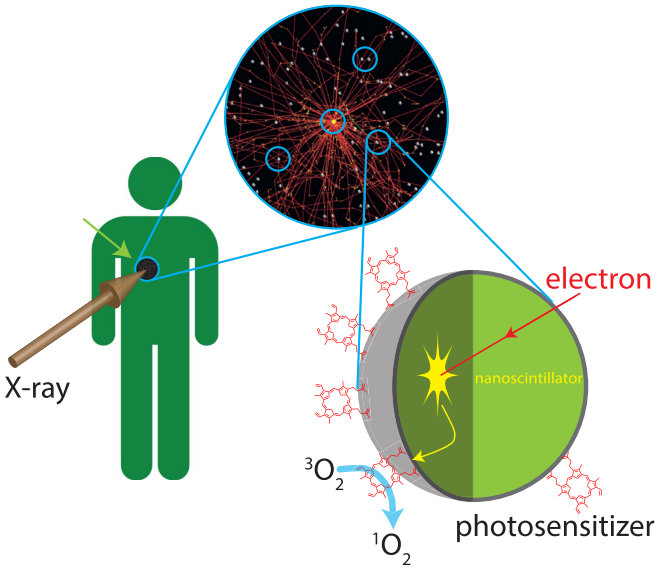

Fig. 8. Concept of photodynamic therapy induced by X-ray during radiotherapy.

purity and doping, such as ZnO:Ga, where defect emission is absent after an appropriate reduction annealing [124]. Exciton confinement effects may also benefit the fast timing issues. Multiple quantum wells of InGaN/GaN have been proposed to obtain ns emission [125]. For the same purpose, lateral confinement effect can speed up the emission [126] and recent works have demonstrated fast response below 1 ns of semiconductor nanoplatelets under X-rays [44]. Another specificity of the nanostructures is the nearfields effects. Already widely studied in the frame of plasmonic fields, optical nanoantenna effect has been demonstrated with X-ray-induced emission, allowing improvement of the directionality of the emission, and a compact dosimeter has been proposed in this framework [127]. Preparation of functional material based on nanostructure is another topic of current research. Core–shell strategy appears very efficient for stabilization of the surface of luminescent-active core that has been used in CdSe-CdS Q-dots and successfully commercially applied in the latest generation of TV screens. Stabilization of the surface of core should bring substantial limitation of trapping states with huge benefit for scintillation efficiency and speed of the response. Furthermore, embedding of Q-dots of direct gap semiconductors into a suitable transparent host can give rise to bulk scintillators with limited reabsorption and superfast scintillation response [124]. Note that radiation hardness has been improved using core-shell architectures [128]. Out of the scintillation field, it has been demonstrated that bulky materials, such as aerogel, superlatices, and even mixture of QDs and lead based-perovskite, can be prepared [129]–[131].

E. Lead-Based Halide Perovskites

Lead halide perovskites have recently emerged in the field of ionizing radiation detectors. Perovskite is a generic term for materials of ABX_3 formula, such as the well-known scintillator $YAlO_3$. When B is Pb and X is a halogen ion, such as Cl,

Br, or I, it leads in most of the cases to a direct bandgap semiconductor. Pb and the halogen atoms are forming octahedra. A is a monovalent cation, generally an organic ammonium or a cesium sitting at the center of the cubes defined by eight PbX_6 units. Depending on the cation steric hindrance, the octahedra planes can be split giving rise to a lamellar structure with multiple quantum well excitonic properties (called 2-D perovskite [132]). Their renewed interest emerged from their photovoltaic performance, reaching recently more than 20% light conversion efficiency [133]. They can be prepared through soft chemistry approaches, as bulk crystals, thin films, or nanoparticles (Q-Dots) are rather easy to process even though they can be quite air sensitive and hygroscopic. Because of their very good charge carrier mobilities, they demonstrate good properties for direct ionizing radiation detection and their preparation cost is considered reasonable as compared to other materials prepared with ultrahigh vacuum techniques. $MaPbI_3$ and $MaPbBr_3$ (Ma for Methylammonium)-based devices have, thus, been prepared as X-ray imaging sensors, and this material is additionally showing very good timing properties as a time response under 10 ps laser excitation down to 340 ns has been achieved [134]. Several other following works have been performed in order to optimize the devices and to demonstrate the spectroscopic capabilities [135], [136]. Similarly, solid solution $MaPbBr_{3x}Cl_x$ perovskite single crystals have demonstrated in charge collection mode an energy resolution about twice that observed with NaI:Tl [137]. Scintillation properties have been demonstrated under 2-MeV protons for the first time on 2-D perovskites [138]. Because of its direct bandgap nature and a high exciton binding energy, $MaPbI_3$ shows a very fast photoluminescence decay [139]. Using four-wave mixing with a fs laser, Kondo *et al.* [140] demonstrated a very fast response of 3.4 ps of the exciton in $(C_6H_{13}NH_3)_2PbI_4$. It has been recently demonstrated that the heterogeneous thin films can exhibit sub-ns cathodoluminescence response [141]. Therefore, in addition to their direct detection capability, lead halide perovskite can also be of great interest for their scintillation properties. It has been shown that the 3-D structure $MAPbX_3$ ($MA = CH_3NH_3$ and X = I, Br, or Cl) sensors in direct detection mode exhibit a thermal quenching at room temperature, leading to a poor scintillation efficiency. On the opposite, the 2-D structure $(EDBE)PbCl_4$ [EDBE = 2, 2-(ethylenedioxy)bis(ethylammonium)] has demonstrated a promising scintillation yield estimated over 120 000 ph/Mev [142]. Because of their small Stokes shift, semiconductors generally suffer for a strong self-absorption. As an illustration, a photon recycling efficiency below 0.5% under sun light excitation has been measured in $MAPbI_3$ and $MAPbBr_3$ single crystal [143]. Nevertheless, lead halide perovskites are a new and emerging family of scintillating materials. They combine scintillation properties with tunable emission wavelength, direct charge collection capability, and show rather fast response.

IV. Material Forms

While material composition impacts light production, the material form plays a key role in light collection. Apart from the performance in terms of stopping power needed in all applications, the light collection aspect plays a major role in imaging and detection systems. The best scintillator becomes useless if appropriate light collection cannot be achieved to reach required spatial resolution, granularity, or spectral resolution. Light collection simulations have already encouraged the development of films, fibers, or structured materials, and even for known composition, a number of synthesis strategies are developed. As an illustration of the progresses in the field of material preparation, printable 3-D structures of the famous YAG:Ce material have been demonstrated [144]. The potential use of such structure is not yet clearly established. Nevertheless, connection between material scientists and end users encouraged in such event as that organized by FAST Cost Action at the SCINT 2017 conference [145] will surely promote new concepts based on this technology and others.

A. Long Inorganic Fibers

A new crystal growth technique has been developed in 1992 by the group of Prof. Fukuda; this so-called micropulling-down technique allows to grow monocrystal fibers of up to 2 m length with a diameter of a typical range of 100 μm–3 mm [146]. In the micropulling-down technique, the raw material melted in a cylindrical crucible enters through a capillary die positioned at the bottom center of the crucible. In contact with a seed, the growth process is started at the bottom of the capillary die by continuously pulling down at a constant pulling rate ranging from 0.1 to 0.5 mm/min (about 10 times faster than Czochralski and 50 times faster than Bridgman). With this technique, crystal fibers of several tens of centimeters can be produced. By modifying the shape of the capillary die, it is possible to produce elongated crystalline materials with noncylindrical cross-sectional geometry. Fibers of different sizes of well-known heavy scintillating crystals, such as BGO, YAG, LuAG, and LSO, can be produced with different diameters and length [147]–[149]. Compared to standard growing methods, the micropulling-down technique allows to grow crystals quite rapidly. Actually, this method was initially used in material research to easily and quickly grow new material samples with small dimensions in order to evaluate their optical properties. More recently, this method gained a new interest due to its suitability for growing long crystal fibers for use in several applications, such as medical imaging and HEP. In medical imaging, crystal pixels of typically $2 \times 2 \times 20$ mm^3 and $3 \times 3 \times 20$ mm^3 are used. Such pixels are, in general, obtained from a large crystal ingot, requiring a significant amount of mechanical treatment with the loss of material at every processing step. With micropulling down, however, it is possible to produce pixels from fibers with already the final section, reducing drastically the amount of mechanical treatment and material loss. In the field of HEP, on the other side, experiments comprising the energy measurement of particles require calorimeters having large volumes compared to medical imaging detectors. Therefore, a cost-effective production of large amounts of detector materials is a key requirement for the detector specification. A new concept of calorimetry was proposed in 2008 [150] for future collider experiments. This approach, based on

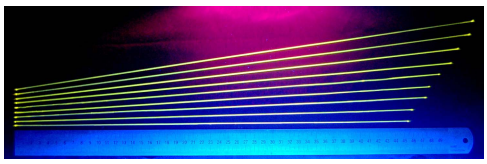

Fig. 9. LuAG:Ce^{3+} fibers produced in ILM Lyon using micropulling-down technique.

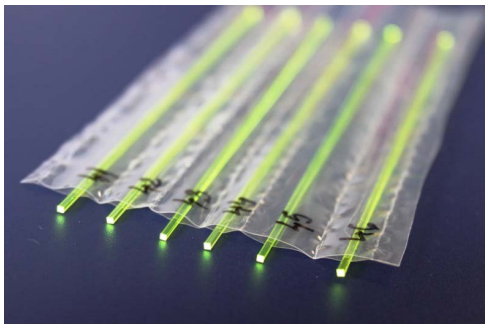

Fig. 10. YAG:Ce square fibers of $1 \times 1 \times 100$ mm^3 produced using fine cutting of large crystal by Crytur company.

metacrystal cables, consists of replacing conventional blocks of scintillating material with bunches of scintillating fibers of dense materials [151], enabling a higher granularity and more flexibility in the detector design [152], [153]. A significant research and development effort has been carried out over the last few years in the frame of the CCC [1] to develop this growing method in order to optimize the production of long-fiber heavy scintillators in view of a future mass production at industrial scale (French ANR project INFINHI [154]), and more recently, a Marie Slowdowska Marie cure RISE project Intelum (grant number 644260) [155]). For heavy crystal fibers, in addition to the more common parameter, such as fast decay time, high scintillation yield, and radiation hardness, this particular shape requires to exhibit a good propagation of the scintillation light within the fiber. In this frame, the garnet composition has been identified as the most promising material [156]. During the last few years, much progress has been made in the understanding and optimization of the growing process and the doping conditions to improve the radial segregation of the dopant, the attenuation length, and the radiation hardness [46], [157], [158] in YAG and LuAG fibers. Long fibers of more than 40-cm length can now be produced in a reproducible way with homogeneous quality in term of light yield and attenuation length (Fig. 9). Further developments are currently carried out in the frame of INTELUM (In Japan Tohoku University and in France Lyon ILM together with IP-ASCR) using a multiple capillary die crucible that allows the simultaneous growth of several fibers in parallel in view of large scale production. Another method to produce crystal fibers has recently been introduced by Crytur (Czech Republic) using fine multiple cutting of square fibers from large size Czochralski-grown crystals of LuAG:Ce and YAG:Ce (Fig. 10). In this case, the length of the fiber is limited by the length of the ingot of about 15 cm up to now. In the latter case, the attenuation length has reached 80 cm.

In addition to crystalline fibers, significant research has been carried out on silica-doped fibers over the last years. These fibers were first developed for remote real-time dosimetry in radiology and radiotherapy [159]–[161]. Scintillation efficiency, linearity upon dose, and signal reproducibility were optimized. These fibers could also be used as an alternative of crystalline fibers for dual readout calorimeters as they emit both Cerenkov and scintillating light when irradiated with high-energy particle beams. In the frame of the Intelum, project developments have been carried out to produce large volume of silica-doped fibers with cerium and praseodymium and to improve the optical properties in terms of scintillation and radiation hardness. It is possible to grow Pr and Ce silica-doped fibers at low cost of more than 20 m and a diameter from 200 to 600 μm with an attenuation length of more than 80 cm [162], [163].

B. Eutectics

Eutectic composites are formed by at least two solid-state phases with nonidentical structures. Each of them demonstrates generally different physical performances. As a result, two or more physical properties can be observed in the same body. The directionally solidified eutectic systems have been discovered in various materials that are considered appropriate for structural and functional applications [164], [165]. Among them, two types of eutectics can be considered for scintillator application. They are for: 1) neutron scintillators; eutectic materials that consist of high neutron cross-sectional material and efficient scintillator (it does not require regular microstructure) and 2) high spatial resolution scintillators; eutectic materials that have well-ordered rod/fiber structure of one of the phases immersed into matrix of second phase (one of them should be efficient scintillator) (see Fig. 11). In the latter one, the wave guiding can be established in one of the phases (either matrix or fibers). The composites with fiber structure are supposed to be very promising substances used for detecting initial irradiation with high spatial resolution competing with the currently used needle-shaped CsI:Tl prepared by evaporation techniques. LiF/$LiYF_4$ and LiF/CaF_2:Eu eutectic composites represent first group of the scintillators [65], [166], [167], but CsI/NaCl and $GdAlO_3$/α-Al_2O_3 correspond to the second one (see Fig. 12) [168], [169].

C. Thin Films

Using highly coherent beams provided by synchrotron facilities, current high resolution X-ray imaging achieves sub-μm spatial resolution. This technique requires scintillators as very thin transparent films (<50 μm) [170]. The X-ray image is generated in the film and enlarged by means of a microscope objective. In order to obtain a good spatial resolution, the image has to be generated within the focus of the objective. Depending on the numerical aperture (NA), the film thickness has, thus, to be lower than a few tens of μm. For a small NA, diffraction limits the resolution. Having thin films limits the stopping power, a key parameter for the acquisition time and the image quality. Dense materials, showing a good scintillation yield, are thus preferred.

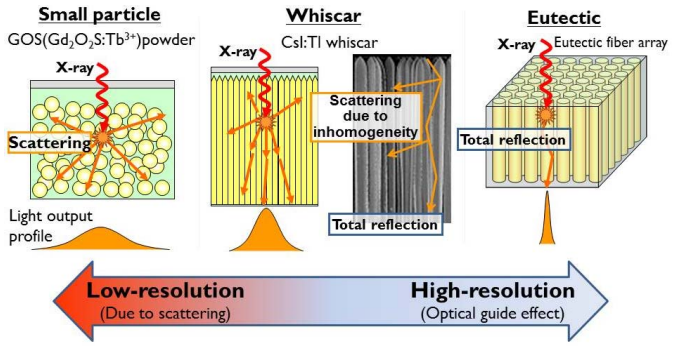

Fig. 11. Expected resolution of three kinds of material state. Small particle gives low resolution due to scattering. Whisker gives higher resolution than that of particles. Highest resolution is expected by the eutectic with optical guide effect.

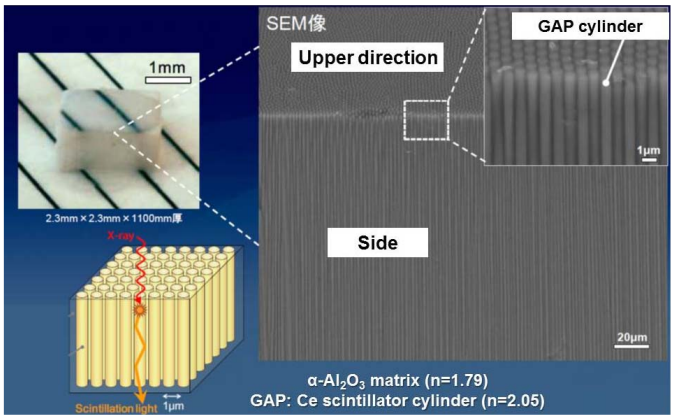

Fig. 12. Ordered structure of the $GdAlO_3/\alpha$-Al_2O_3 eutectic composites according to scanning electron microscopy.

The lowest afterglow is required in order to allow high repetition rate as needed in the case of tomography. Such thin films generally require substrates, and because the films absorb only about 5% of the X-ray beam, most of it is absorbed in the substrate. It requires to use nonscintillating substrate that prevents the generation of a signal out of focus that can blur the image. There are several synthesis methods to prepare thin films, all of them having their own accessible range of thickness and substrate requirement: sol–gel coating, liquid-phase epitaxy, and chemical-vapor deposition. Several garnet-, perovskite-, and silicate-based thin films have been successfully grown using liquid-phase epitaxy for this purpose [171]. Strategies to improve X-ray absorption while keeping the spatial resolution have been developed. Combining two films of different scintillators emitting at different wavelength has been proposed with LSO:Tb^{3+} and LYSO:Ce^{3+} [172]. Ultra-dense materials, such as Lu_2O_3:Eu^{3+} sesquioxyde, have been recently developed [173]–[175]. This approach is material limited. In addition to the density, the X-ray energy absorption coefficient strongly depends on the K-edge energy of the element composing the films. Adapting the K-edge to the energy of the X-ray has been demonstrated with gadolinium- and lutetium-based aluminum perovskites [176]. In order to overcome the diffraction limit, inspired by the stimulated emission depletion technique developed in optical microscopy imaging, recent works on stimulated scintillation emission depletion have been published [177], [178]. The depletion effect has been successfully observed, and first imaging tests demonstrated. Beam position monitors are also requiring thin films. The goal is to obtain online information about the synchrotron beam while preserving it, in order to correct experimental results from intensity, position, and beam shape fluctuations. The thin films quality criteria are the same as for high resolution X-ray imaging except that the overall X-ray absorption has to be kept below about 10%. Pulsed laser deposition on porous alumina membrane has shown very good performances [179]. The needs are currently focusing on the X-ray absorption efficiency. As described earlier, the strategy is to adapt the material composition regarding the K-edge of the elements. The stability of the scintillation response is also crucial in order to obtain quantitative information. Afterglow, radiation damages, and bright-burn, have to be minimal. More and more experiments are performed with high flux, which has an impact not only on the film aging but also on the operation temperature. The yield has to be, thus, stable at elevated temperatures.

V. Theory and Modeling

General scheme of the scintillation processes was well developed during the last 50 years. However, the needs arisen in the last decade demand deeper understanding of these processes. The enhancement of energy resolution is among these demands. One of the causes of energy resolution limitation is the nonproportional response of most scintillators. Therefore, there have been significant efforts to investigate this problem both experimentally and theoretically. Another demand is for scintillating materials with fast decay of their luminescence.

Theoretical investigations of the processes in scintillators deal with different stages of energy relaxation and transfer in wideband inorganic crystals. It is well-known that these stages are interrelated, and the modern view of formation of the scintillator response is described in [180] and [181]. During the last few years, a lot of attention was paid to the formation of the spatial distribution of electrons and holes, which is mostly controlled by the thermalization stage following the cascade of the production of new excitations. This stage is responsible not only for the creation of overall spatial distribution but also for emerging electric fields due to the separation of electron and hole. Thermalization stage is controlled by interaction of hot carriers with kinetic energy below the forbidden gap energy with phonons. Simple effective mass models are shown to be not applicable for the description of electron–phonon interaction and even for the prediction of group velocities of carriers with sufficient kinetic energy, so great attention was paid to the description of these properties in real crystals with complicated band structures [86], [182]–[184]. In general, effective mass approximation results in overestimation of the thermalization length in most crystals since group velocities and mobilities of hot carriers are overestimated. A set of papers are devoted

to the description of the next stage, namely, the interaction and the recombination of charge carriers, which are described using either classical rate equations [185]–[187] or kinetic Monte Carlo calculations [188], [189]. This approach to thermalization stage makes a further step toward developing a toolkit to estimate scintillators properties [186]. We should also mention efficient techniques for simulation developed by the group from the Pacific Northwest National Laboratory, USA, and their collaborators. They develop a set of tools, including calculation of elementary cross sections and momentum-dependent energy loss functions, high-energy Monte Carlo simulation of the cascade, simulation of the thermalization, and finally a package for kinetic Monte Carlo simulation of the final relaxation stage involving recombination and luminescence [188]–[190]. Unfortunately, these calculations are hardly scalable to high energies of ionizing particles and are very specific for different materials, so simplified approaches, such as [63], could be useful as well. Such theoretical studies are directed not only to deeper understanding of fundamental processes in scintillators but also attempt to elucidate the origin of nonproportionality and to discover ways to improve energy resolution of scintillators. Recent experimental investigations of energy resolution for different shaping times [87], [191] and previous Scintillation Light Yield Non-proportionality Characterization Instrument experiments became a motivation for deeper development of phenomenological models of nonproportionality [192]–[194] together with microscopic models that simulate the decay kinetics and scintillation yield under excitation by γ photons with different energies [87], [191], [195]–[197]. The role of large-scale Landau fluctuations in tracks and their effect on the energy resolution are analyzed in [198]. The revival of interest in picosecond intraband luminescence, a process competing with thermalization, was triggered by the study of the thermalization of hot excitations and the recent need for ultrafast scintillators. Experimental and theoretical investigations [199], [200] were stimulated by the European TICAL ERC Advanced Grant Project [201] and the COST FAST Program [202]. It was shown that intraband luminescence is most pronounced in the crystals with very low-energy optical phonons and in the systems with strongly nonuniform density of states [17]. Most of the novel scintillators are not simple crystals but solid solutions that show enhanced scintillation yield [203]. One of the possible explanations of such behavior of solid solutions is the lower thermalization length due to spatial fluctuations of the band edges [204]. Limitation of spatial dimensions plays a critical role especially in case of nanoparticles. The luminescence yield of nanoparticles under γ and X-ray irradiation is seriously decreased if nanoparticle size becomes comparable with mean free path of primary electrons [118] or with thermalization length of hot electrons [205], [206]. The advances in quantum chemistry calculations in material science and availability of modern computer resources result in exponential growth of papers devoted to band structure calculations of ideal crystals and crystals with defects and activators. Now, there are about one and a half million electronic band structures of crystals in AFLOW database [207], [208], which is very useful as the first estimation of electronic properties of new scintillators. Definitely, much more reliable investigations were made for different first-principles calculations of specific crystals (see [209] as an example). Fairly good progress was achieved in first-principles calculation of activators, both rare earth ions (see [210] and [211]) and heavy ions [212], [213]. First-principle calculations make a step toward obtaining not only positions of energy levels, but some dynamical parameters, such as multiphonon capture and recombination rates [214]–[216], the parameters that are very important for reliable application of above-mentioned calculations using rate equations or kinetic Monte Carlo schemes. Nevertheless, spectroscopic accuracy even of defect level positions is not achieved yet.

VI. Conclusion

After decades of research on scintillating materials, we can conclude that the field has deeply changed, as shown in the recent handbook [217]. The evolution stems from multidisciplinary approaches tuned to the needs of specific field of applications. In this context, each subfield is still very active and variety of applications is continuously enriched. The needs of the end users are permanently changing. They also benefit from progress in other fields, such as photodetectors, signal processing, computing, or data-flow capacity. On the other side, the material science technologies have been greatly developed and stimulated by other emerging applications. Further progress and deeper understanding require to link and gather these opposite sides. Such a link requires deep theoretical studies of complex schemes of the relaxation paths of energy occurring in scintillator and description of its electronic band structure, including atomistic irregularities. From the experimental side, more extended and correlated techniques are needed for the detailed description of luminescence and scintillation characteristics in a broad range of external parameters as temperature, excitation energy, and time domain. Experimental description and understanding of the defects and related charge traps acting in scintillation mechanism and their relation to manufacturing technology are also of critical importance. The scintillation science has thus emerged.

Acknowledgment

The authors would like to thank the SCINT conference series community.

References

[1] [Online]. Available: http://crystalclear.web.cern.ch/crystalclear/
[2] [Online]. Available: http://scint.univ-lyon1.fr
[3] S. E. Derenzo *et al.*, "Design and implementation of a facility for discovering new scintillator materials," *IEEE Trans. Nucl. Sci.*, vol. 55, no. 3, pp. 1458–1463, Jun. 2008.
[4] [Online]. Available: http://scintillator.lbl.gov/
[5] C. W. E. van Eijk, "Inorganic scintillators for thermal neutron detection," *Radiat. Meas.*, vol. 38, nos. 4–6, pp. 337–342, Aug. 2004.
[6] E. D. Bourret-Courchesne *et al.*, "Eu^{2+}-doped Ba_2CsI_5, a new high-performance scintillator," *Nucl. Instrum. Methods Phys. Res. A, Accel. Spectrom. Detect. Assoc. Equip.*, vol. 612, no. 1, pp. 138–142, Dec. 2009.
[7] E. D. Bourret-Courchesne, G. Bizarri, S. M. Hanrahan, G. Gundiah, Z. Yan, and S. E. Derenzo, "BaBrI:Eu^{2+}, a new bright scintillator," *Nucl. Instrum. Methods Phys. Res. A, Accel. Spectrom. Detect. Assoc. Equip.*, vol. 613, no. 1, pp. 95–97, Jan. 2010.

[8] G. Bizarri, E. D. Bourret-Courchesne, Z. Yan, and S. E. Derenzo, "Scintillation and optical properties of BaBrI:Eu^{2+} and $CsBa_2I_5$:Eu^{2+}," *IEEE Trans. Nucl. Sci.*, vol. 58, no. 6, pp. 3403–3410, Dec. 2011.

[9] N. J. Cherepy *et al.*, "SrI_2 scintillator for gamma ray spectroscopy," *Proc. SPIE, Hard X-Ray, Gamma-Ray, Neutron Detect. Phys. XI*, vol. 7449, p. 74490F, Sep. 2009, doi: 10.1117/12.830016.

[10] N. Shiran *et al.*, "Modification of Nai crystal scintillation properties by Eu-doping," *Opt. Mater.*, vol. 32, no. 10, pp. 1345–1348, Aug. 2010.

[11] K. Yang and P. R. Menge, "Improving γ-ray energy resolution, non-proportionality, and decay time of NaI:Tl^+ with Sr^{2+} and Ca^{2+} co-doping," *J. Appl. Phys.*, vol. 118, no. 21, p. 213106, Dec. 2015.

[12] I. V. Khodyuk, S. A. Messina, T. J. Hayden, E. D. Bourret, and G. A. Bizarri, "Optimization of scintillation performance via a combinatorial multi-element co-doping strategy: Application to NaI:Tl," *J. App. Phys.*, vol. 118, iss. 8, p. 084901, Aug. 2015.

[13] P. Lebrun *et al.*, Eds.,"The CLIC programme: Towards a staged e^+e^- linear collider exploring the terascale," CERN, Geneva, Switzerland, Tech. Rep. CERN-2012-005, 2012.

[14] The CMS Collaboration, "Technical proposal for the phase-II upgrade of the CMS detector," CERN, Geneva, Switzerland, Tech. Rep. CERN-LHCC-2015-010/LHCC-P-008, 2015.

[15] M. Conti, "State of the art and challenges of time-of-flight PET," *Phys. Med.*, vol. 25, no. 1, pp. 1–11, Mar. 2009.

[16] T. F. Budinger, "Time-of-flight positron emission tomography: Status relative to conventional PET," *J. Nucl. Med.*, vol. 24, no. 1, pp. 73–78, Jan. 1983.

[17] P. Lecoq, "Pushing the limits in time-of-flight PET imaging," *IEEE Trans. Radiat. Plasma Med. Sci.*, vol. 1, no. 6, pp. 473–485, Nov. 2017.

[18] K. Parodi, F. Ponisch, and W. Enghardt, "Experimental study on the feasibility of in-beam PET for accurate monitoring of proton therapy," *IEEE Trans. Nucl. Sci.*, vol. 52, no. 3, pp. 778–786, Jun. 2005.

[19] Y. Shao, "A new timing model for calculating the intrinsic timing resolution of a scintillator detector," *Phys. Med. Biol.*, vol. 52, no. 4, p. 1103, 2007.

[20] P. Lecoq *et al.*, "Factors influencing time resolution of scintillators and ways to improve them," in *Proc. IEEE Nucl. Sci. Symp. Conf. Rec. (NSS/MIC)*, Oct. 2009, pp. 1880–1885.

[21] P. Lecoq, M. Korzhik, and A. Vasiliev, "Can transient phenomena help improving time resolution in scintillators?" *IEEE Trans. Nucl. Sci.*, vol. 61, no. 1, pp. 229–234, Feb. 2014.

[22] C. W. Barnes *et al.*, "Technology risk mitigation research and development for the matter-radiation interactions in extremes (MARIE) project," Los Alamos Nat. Lab., Los Alamos, NM, USA, Tech. Rep. LA-UR-17-26474, 2017.

[23] P. Denes, S. Gruner, M. Stevens, and Z. Wang, "Ultrafast and high-energy X-ray imaging technologies and applications," Los Alamos Nat. Lab., Los Alamos, NM, USA, Tech. Rep. LA-UR-17-22085, 2017.

[24] Z. Wang *et al.*, "Thin scintillators for ultrafast hard X-ray imaging," *Proc. SPIE, Photon Counting Appl.*, vol. 9504, p. 95040N, May 2015, doi: 10.1117/12.2178420.

[25] R.-Y. Zhu, "Very fast inorganic crystal scintillators," *Proc. SPIE, Hard X-Ray, Gamma-Ray, Neutron Detect. Phys. XIX*, vol. 10392, p. 103920G, Sep. 2017, doi: 10.1117/12.2274617.

[26] M. Prange, D. Wu, Y. Xie, L. W. Campbell, F. Gao, and S. Kerisit, *Radiation Response of Inorganic Scintillators: Insights From Monte Carlo Simulations*, A. Burger, L. Franks, R. B. James, and M. Fiederle, Eds. 2014, p. 92130L.

[27] P. Lecoq, "The 10 ps timing-of-flight pet challenge," presented at the Conf. Inorganic Scintillators Appl. (SCINT), Chamonix, France, 2017.

[28] R.-Y. Zhu, "Applications of very fast inorganic crystal scintillators for future HEP experiments," presented at the Conf. Inorganic Scintillators Appl. (SCINT), Chamonix, France 2017.

[29] J. S. Carlson, P. Marleau, R. A. Zarkesh, and P. L. Feng, "Taking advantage of disorder: Small-molecule organic glasses for radiation detection and particle discrimination," *J. Amer. Chem. Soc.*, vol. 139, no. 28, pp. 9621–9626, Jul. 2017.

[30] R.-Y. Zhu, "The next generation of crystal detectors," *Radiat. Detection Technol. Methods*, vol. 2, no. 1, p. 2, Jun. 2018.

[31] S. Chatrchyan *et al.*, "Observation of a new boson at a mass of 125 GeV with the CMS experiment at the LHC," *Phys. Lett. B*, vol. 716, no. 1, pp. 30–61, 2012.

[32] T. T. de Fatis, "Role of the CMS electromagnetic calorimeter in the hunt for the Higgs boson in the two-gamma channel," *J. Phys., Conf. Ser.*, vol. 404, p. 012002, Dec. 2012.

[33] R.-Y. Zhu, "Radiation damage in scintillating crystals," *Nucl. Instrum. Methods Phys. Res. A, Accel. Spectrom. Detect. Assoc. Equip.*, vol. 413, nos. 2–3, pp. 297–311, Aug. 1998.

[34] A. N. Annenkov *et al.*, "Systematic study of the short-term instability of PBWO-4 scintillator parameters under irradiation," *Radiat. Meas.*, vol. 29, no. 1, pp. 27–38, Feb. 1998.

[35] R.-Y. Zhu, "A very compact crystal shashlik electromagnetic calorimeter for future HEP experiments," *J. Phys., Conf. Ser.*, vol. 928, p. 012015, Nov. 2017.

[36] F. Yang, L. Zhang, and R.-Y. Zhu, "Gamma-ray induced radiation damage up to 340 Mrad in various scintillation crystals," *IEEE Trans. Nucl. Sci.*, vol. 63, no. 2, pp. 612–619, Apr. 2016.

[37] M. T. Lucchini *et al.*, "Effect of Mg^{2+} ions co-doping on timing performance and radiation tolerance of cerium doped $Gd_3Al_2Ga_3O_{12}$ crystals," *Nucl. Instrum. Methods Phys. Res. A, Accel. Spectrom. Detect. Assoc. Equip.*, vol. 816, pp. 176–183, Apr. 2016.

[38] M. T. Lucchini, K. Pauwels, K. Blazek, S. Ochesanu, and E. Auffray, "Radiation tolerance of LuAG:Ce and YAG:Ce crystals under high levels of gamma- and proton-irradiation," *IEEE Trans. Nucl. Sci.*, vol. 63, no. 2, pp. 586–590, Apr. 2016.

[39] F. Yang, L. Zhang, R.-Y. Zhu, J. Kapustinsky, R. Nelson, and Z. Wang, "Proton-induced radiation damage in fast crystal scintillators," *IEEE Trans. Nucl. Sci.*, vol. 64, no. 1, pp. 665–672, Jan. 2017.

[40] C. Hu *et al.*, "Neutron-induced radiation damage in BaF_2, LYSO and PWO crystals," presented at the Conf. Inorganic Scintillators Appl., Chamonix, France, 2017.

[41] T. T. de Fatis, "Studies of precision time-tagging of charged tracks with scintillating crystals for the phase-II upgrade of CMS," presented at the Conf. Inorganic Scintillators Appl. (SCINT), Chamonix, France, 2017.

[42] [Online]. Available: https://indico.hep.anl.gov/indico/conferenceDisplay.py?ovw=True&confId=1258

[43] J. Chen *et al.*, "Slow scintillation suppression in yttrium doped BaF_2 crystals," *IEEE Trans. Nucl. Sci.*, to be published, doi: 10.1109/TNS.2017.2786042.

[44] R. M. Turtos *et al.*, "Ultrafast emission from colloidal nanocrystals under pulsed X-ray excitation," *J. Instrum.*, vol. 11, no. 10, p. P10015, Oct. 2016.

[45] A. Driutti, A. Para, G. Pauletta, N. R. Briones, and H. Wenzel, "Towards jet reconstruction in a realistic dual readout total absorption calorimeter," *J. Phys., Conf. Ser.*, vol. 293, p. 012034, Apr. 2011.

[46] K. Pauwels *et al.*, "Single crystalline LuAG fibers for homogeneous dual-readout calorimeters," *J. Instrum.*, vol. 8, no. 9, p. P09019, 2013.

[47] R. Mao, L. Zhang, and R. Y. Zhu, "Crystals for the HHCAL detector concept," *IEEE Trans. Nucl. Sci.*, vol. 59, no. 5, pp. 2229–2236, Oct. 2012.

[48] M. Lucchini *et al.*, "Scintillation properties and radiation tolerance of Alkali Free Fluorophosphate Glasses with different dopant concentrations," in *Proc. Int. Conf. Inorganic Scintillators Appl. (SCINT)*, Chamonix, France, 2017.

[49] C. Hu *et al.*, "Alkali-free ce-doped and co-doped fluorophosphate glasses for future hep experiments," presented at the IEEE NSS/MIC Conf., Atlanta, GA, USA, 2017.

[50] K. E. Mesick, D. D. S. Coupland, and L. C. Stonehill, "Pulse-shape discrimination and energy quenching of alpha particles in $Cs_2LiLaBr_6$:Ce^{3+}," *Nucl. Instrum. Methods Phys. Res. A, Accel. Spectrom. Detect. Assoc. Equip.*, vol. 841, pp. 139–143, Jan. 2017.

[51] N. D'Olympia *et al.*, "Pulse-shape analysis of CLYC for thermal neutrons, fast neutrons, and gamma-rays," *Nucl. Instrum. Methods Phys. Res. A, Accel. Spectrom. Detect. Assoc. Equip.*, vol. 714, pp. 121–127, Jun. 2013.

[52] W. Wolszczak and P. Dorenbos, "Shape of intrinsic alpha pulse height spectra in lanthanide halide scintillators," *Nucl. Instrum. Methods Phys. Res. A, Accel. Spectrom. Detect. Assoc. Equip.*, vol. 857, pp. 66–74, Jun. 2017.

[53] V. Gayshan, A. Gektin, S. Vasyukov, S. Gridin, D. Onken, and R. Williams, "Pulse shape analysis of individual gamma events—Correlation to resolution and the possibility of its improvement," presented at the 14th Int. Conf. Scintillating Mater. Appl., 2017.

[54] J. Czochralski, "Ein neues Verfahren zur Messung der Kristallisationsgeschwindigkeit der Metalle," *Zeitschrift Physikalische Chemie*, vol. 92U, no. 1, pp. 219–221, Jan. 1918.

[55] A. Yoshikawa *et al.*, "Crystal growth and scintillation properties of multi-component oxide single crystals: Ce:GGAG and Ce:La-GPS," *J. Lumin.*, vol. 169, pp. 387–393, Jan. 2016.

[56] K. Kamada *et al.*, "Scintillator-oriented combinatorial search in Ce-doped $(Y,Gd)_3(Ga,Al)_5O_{12}$ multicomponent garnet compounds," *J. Phys. D, Appl. Phys.*, vol. 44, no. 50, p. 505104, Dec. 2011.

[57] M. Nikl *et al.*, "Development of LuAG-based scintillator crystals—A review," *Prog. Cryst. Growth Characterization Mater.*, vol. 59, no. 2, pp. 47–72, Jun. 2013.

[58] K. Kamada *et al.*, "Growth and scintillation properties of 3 in. diameter Ce doped $Gd_3Ga_3Al_2O_{12}$ scintillation single crystal," *J. Cryst. Growth*, vol. 452, pp. 81–84, Oct. 2016.

[59] K. Kamada *et al.*, "2 inch size Czochralski growth and scintillation properties of Li^+ co-doped Ce:$Gd_3Ga_3Al_2O_{12}$," *Opt. Mater.*, vol. 65, pp. 52–55, Mar. 2017.

[60] K. Kamada *et al.*, "Single crystal growth of Ce:$Gd_3(Ga,Al)_5O_{12}$ with various Mg concentration and their scintillation properties," *J. Cryst. Growth*, vol. 468, pp. 407–410, Jun. 2017.

[61] G. Tamulaitis *et al.*, "Subpicosecond luminescence rise time in magnesium codoped GAGG:Ce scintillator," *Nucl. Instrum. Methods Phys. Res. A, Accel. Spectrom. Detect. Assoc. Equip.*, vol. 870, pp. 25–29, Oct. 2017.

[62] [Online]. Available: http://www.c-and-a.jp/products.html

[63] A. Gektin, S. Vasyukov, E. Galenin, V. Taranyuk, N. Nazarenko, and V. Romanchuk, "Strontium iodide: Technology aspects of raw material choice and crystal growth," *Funct. Mater.*, vol. 23, no. 3, pp. 473–477, Jan. 2016.

[64] E. Galenin, O. Sidletskiy, C. Dujardin, and A. Getkin, "Growth and characterization of SrI_2:Eu crystals fabricated by the Czochralski method," *IEEE Trans. Nucl. Sci.*, to be published, doi: 10.1109/TNS.2017.2787420.

[65] Y. Yokota, S. Kurosawa, K. Nishimoto, K. Kamada, and A. Yoshikawa, "Growth of Eu:SrI_2 bulk crystals and their scintillation properties," *J. Cryst. Growth*, vol. 401, pp. 343–346, Sep. 2014.

[66] A. C. Lindsey, Y. Wu, M. Zhuravleva, M. Loyd, M. Koschan, and C. L. Melcher, "Multi-ampoule Bridgman growth of halide scintillator crystals using the self-seeding method," *J. Cryst. Growth*, vol. 470, pp. 20–26, Jul. 2017.

[67] Z. Yan, T. Shalapska, and E. D. Bourret, "Czochralski growth of the mixed halides BaBrCl and BaBrCl:Eu," *J. Cryst. Growth*, vol. 435, pp. 42–45, Feb. 2016.

[68] R. Apetz and M. P. B. van Bruggen, "Transparent alumina: A light-scattering model," *J. Amer. Ceram. Soc.*, vol. 86, no. 3, pp. 480–486, Mar. 2003.

[69] M. Nikl, T. Yanagida, H. Yagi, T. Yanagitani, E. Mihokova, and A. Yoshikawa, "Optical ceramics for fast scintillator materials," in *Recent Advances in Ceramic Materials Research*, J. J. R. Rovira and M. S. Rubi, Eds. Commack, NY, USA: Nova, 2013, pp. 127–176.

[70] N. J. Cherepy *et al.*, "High energy resolution with transparent ceramic garnet scintillators," *Proc. SPIE, Hard X-Ray, Gamma-Ray, Neutron Detect. Phys. XVI*, vol. 9213, p. 921302, Sep. 2014, doi: 10.1117/12.2062959.

[71] F. Moretti *et al.*, "Thermoluminescence evidence of grain boundary structural disorder in LuAG:Ce optical ceramics," presented at the Conf. Inorganic Scintillators Appl. (SCINT), Chamonix, France, 2017.

[72] S. R. Podowitz, R. M. Gaume, W. T. Hong, A. Laouar, and R. S. Feigelson, "Fabrication and properties of translucent SrI_2 and Eu:SrI_2 scintillator ceramics," *IEEE Trans. Nucl. Sci.*, vol. 57, no. 6, pp. 3827–3835, Dec. 2010.

[73] W. Shoulders, "Stress-induced phase change sintering: A novel approach to the fabrication of barium chloride transparent ceramic scintillators," Ph.D. dissertation, Dept. Mater. Sci. Eng., Univ. Central Florida, Orlando, FL, USA, 2016.

[74] H. Yamada, A. Suzuki, Y. Uchida, M. Yoshida, H. Yamamoto, and Y. Tsukuda, "A scintillator Gd_2O_2S:Pr, Ce, F for X-ray computed tomography," *J. Electrochem. Soc.*, vol. 136, no. 9, pp. 2713–2716, 1989.

[75] S. J. Duclos *et al.*, "Development of the HiLight scintillator for computed tomography medical imaging," *Nucl. Instrum. Methods Phys. Res. A, Accel. Spectrom. Detect. Assoc. Equip.*, vol. 505, nos. 1–2, pp. 68–71, Jun. 2003.

[76] M. Nikl, "Wide band gap scintillation materials: Progress in the technology and material understanding," *Phys. Status Solidi A*, vol. 178, no. 2, pp. 595–620, Apr. 2000.

[77] A. A. Annenkov, M. V. Korzhik, and P. Lecoq, "Lead tungstate scintillation material," *Nucl. Instrum. Methods Phys. Res. A, Accel. Spectrom. Detect. Assoc. Equip.*, vol. 490, nos. 1–2, pp. 30–50, Sep. 2002.

[78] L. Nagornaya *et al.*, "Production of the high-quality $CdWO_4$ single crystals for application in CT and radiometric monitoring," *Nucl. Instrum. Methods Phys. Res. A, Accel. Spectrom. Detect. Assoc. Equip.*, vol. 537, nos. 1–2, pp. 163–167, Jan. 2005.

[79] M. Buryi, V. V. Laguta, J. Hybler, M. Nikl, and J. Rosa, "Electron spin resonance investigation of undoped and Li-doped $CdWO_4$ scintillator crystals," *Phys. Status Solidi B*, vol. 248, no. 4, pp. 993–996, Apr. 2011.

[80] M. S. Alekhin, D. A. Biner, K. W. Krämer, and P. Dorenbos, "Improvement of $LaBr_3$:5%Ce scintillation properties by Li^+, Na^+, Mg^{2+}, Ca^{2+}, Sr^{2+}, and Ba^{2+} co-doping," *J. Appl. Phys.*, vol. 113, no. 22, p. 224904, Jun. 2013.

[81] M. S. Alekhin *et al.*, "Improvement of γ-ray energy resolution of $LaBr_3$:Ce^{3+} scintillation detectors by Sr^{2+} and Ca^{2+} co-doping," *Appl. Phys. Lett.*, vol. 102, no. 16, p. 161915, Apr. 2013.

[82] D. Åberg, B. Sadigh, A. Schleife, and P. Erhart, "Origin of resolution enhancement by co-doping of scintillators: Insight from electronic structure calculations," *Appl. Phys. Lett.*, vol. 104, no. 21, p. 211908, May 2014.

[83] G. Bizarri, W. W. Moses, J. Singh, A. N. Vasil'ev, and R. T. Williams, "An analytical model of nonproportional scintillator light yield in terms of recombination rates," *J. Appl. Phys.*, vol. 105, no. 4, p. 044507, 2009.

[84] Q. Li *et al.*, "Host structure dependence of light yield and proportionality in scintillators in terms of hot and thermalized carrier transport," *Phys. Status Solidi (RRL) Rapid Res. Lett.*, vol. 6, no. 8, pp. 346–348, Aug. 2012.

[85] J. Q. Grim *et al.*, "Nonlinear quenching of densely excited states in wide-gap solids," *Phys. Rev. B, Condens. Matter*, vol. 87, p. 125117, Mar. 2013.

[86] K. B. Ucer, G. Bizarri, A. Burger, A. Gektin, L. Trefilova, and R. T. Williams, "Electron thermalization and trapping rates in pure and doped alkali and alkaline-earth iodide crystals studied by picosecond optical absorption," *Phys. Rev. B, Condens. Matter*, vol. 89, no. 16, p. 165112, Apr. 2014.

[87] X. Lu *et al.*, "Energy-dependent scintillation pulse shape and proportionality of decay components for CsI:Tl: Modeling with transport and rate equations," *Phys. Rev. Appl.*, vol. 7, no. 1, p. 014007, Jan. 2017.

[88] C. Brecher *et al.*, "Suppression of afterglow in CsI:Tl by codoping with Eu^{2+}—I: Experimental," *Nucl. Instrum. Methods Phys. Res. A, Accel. Spectrom. Detect. Assoc. Equip.*, vol. 558, no. 2, pp. 450–457, Mar. 2006.

[89] R. H. Bartram *et al.*, "Suppression of afterglow in CsI:Tl by codoping with Eu^{2+}—II: Theoretical model," *Nucl. Instrum. Methods Phys. Res. A, Accel. Spectrom. Detect. Assoc. Equip.*, vol. 558, no. 2, pp. 458–467, Mar. 2006.

[90] V. V. Nagarkar *et al.*, "Scintillation properties of CsI:Tl crystals codoped with Sm^{2+}," *IEEE Trans. Nucl. Sci.*, vol. 55, no. 3, pp. 1270–1274, Jun. 2008.

[91] D. Totsuka *et al.*, "Afterglow suppression by codoping with Bi in CsI:Tl crystal scintillator," *Appl. Phys. Express*, vol. 5, no. 5, p. 52601, 2012.

[92] Y. Wu *et al.*, "Effects of Bi^{3+} codoping on the optical and scintillation properties of CsI:Tl single crystals," *Phys. Status Solidi A*, vol. 211, no. 11, pp. 2586–2591, Nov. 2014.

[93] Y. Wu *et al.*, "CsI:Tl^+,Yb^{2+}: Ultra-high light yield scintillator with reduced afterglow," *CrystEngComm*, vol. 16, no. 16, pp. 3312–3317, 2014.

[94] M. A. Spurrier, P. Szupryczynski, K. Yang, A. A. Carey, and C. L. Melcher, "Effects of Ca^{2+} Co-doping on the scintillation properties of LSO:Ce," *IEEE Trans. Nucl. Sci.*, vol. 55, no. 3, pp. 1178–1182, Jun. 2008.

[95] K. Yang, C. L. Melcher, P. D. Rack, and L. A. Eriksson, "Effects of calcium codoping on charge traps in LSO:Ce crystals," *IEEE Trans. Nucl. Sci.*, vol. 56, no. 5, pp. 2960–2965, Oct. 2009.

[96] H. E. Rothfuss, C. L. Melcher, L. A. Eriksson, and M. A. S. Koschan, "The effect of Ca^{2+} codoping on shallow traps in YSO:Ce scintillators," *IEEE Trans. Nucl. Sci.*, vol. 56, no. 3, pp. 958–961, Jun. 2009.

[97] S. Blahuta, A. Bessière, B. Viana, P. Dorenbos, and V. Ouspenski, "Evidence and Consequences of Ce^{4+} in LYSO:Ce,Ca and LYSO:Ce,Mg single crystals for medical imaging applications," *IEEE Trans. Nucl. Sci.*, vol. 60, no. 4, pp. 3134–3141, Aug. 2013.

[98] M. Nikl *et al.*, "Defect engineering in ce-doped aluminum garnet single crystal scintillators," *Cryst. Growth Des.*, vol. 14, no. 9, pp. 4827–4833, Sep. 2014.

[99] S. P. Liu, X. Q. Feng, Z. W. Zhou, M. Nikl, Y. Shi, and Y. B. Pan, "Effect of Mg^{2+} co-doping on the scintillation performance of LuAG:Ce ceramics," *Phys. Status Solidi RRL*, vol. 8, no. 1, pp. 105–109, Jan. 2014.

[100] M. Nikl and A. Yoshikawa, "Recent R&D trends in inorganic single-crystal scintillator materials for radiation detection," *Adv. Opt. Mater.*, vol. 3, no. 4, pp. 463–481, Apr. 2015.

[101] K. Kamada *et al.*, "Alkali earth co-doping effects on luminescence and scintillation properties of Ce doped $Gd_3Al_2Ga_3O_{12}$ scintillator," *Opt. Mater.*, vol. 41, pp. 63–66, Mar. 2015.

[102] M. Lucchini *et al.*, "Timing capabilities of garnet crystals for detection of high energy charged particles," *Nucl. Instrum. Methods Phys. Res. A, Accel. Spectrom. Detect. Assoc. Equip.*, vol. 852, pp. 1–9, Apr. 2017.

[103] F. Moretti *et al.*, "Consequences of Ca codoping in $YAlO_3$:Ce single crystals," *ChemPhysChem*, vol. 18, no. 5, pp. 493–499, Mar. 2017.

[104] J. Pejchal *et al.*, "Luminescence and scintillation properties of Mg-codoped LuAG:Pr single crystals annealed in air," *J. Lumin.*, vol. 181, pp. 277–285, Jan. 2017.

[105] S. E. Létant and T.-F. Wang, "Semiconductor quantum dot scintillation under γ-ray irradiation," *Nano Lett.*, vol. 6, no. 12, pp. 2877–2880, Dec. 2006.

[106] C. Dujardin, D. Amans, A. Belsky, F. Chaput, G. Ledoux, and A. Pillonnet, "Luminescence and scintillation properties at the nanoscale," *IEEE Trans. Nucl. Sci.*, vol. 57, no. 3, pp. 1348–1354, Jun. 2010.

[107] E. A. McKigney *et al.*, "Nanocomposite scintillators for radiation detection and nuclear spectroscopy," *Nucl. Instrum. Methods Phys. Res. A, Accel. Spectrom. Detect. Assoc. Equip.*, vol. 579, no. 1, pp. 15–18, Aug. 2007.

[108] Z. T. Kang *et al.*, "$GdBr_3$:Ce in glass matrix as nuclear spectroscopy detector," *Radiat. Meas.*, vol. 48, pp. 7–11, Jan. 2013.

[109] P. Guss *et al.*, "Lanthanum halide nanoparticle scintillators for nuclear radiation detection," *J. Appl. Phys.*, vol. 113, no. 6, p. 064303, May 2013.

[110] Z. Kang *et al.*, "CdTe quantum dots and polymer nanocomposites for X-ray scintillation and imaging," *Appl. Phys. Lett.*, vol. 98, no. 18, p. 181914, 2011.

[111] C. Liu, Z. Li, T. J. Hajagos, D. Kishpaugh, D. Y. Chen, and Q. Pei, "Transparent ultra-high-loading quantum dot/polymer nanocomposite monolith for gamma scintillation," *ACS Nano*, vol. 11, no. 6, pp. 6422–6430, Jun. 2017.

[112] L. Winslow and R. Simpson, "Characterizing quantum-dot-doped liquid scintillator for applications to neutrino detectors," *J. Instrum.*, vol. 7, no. 7, p. P07010, Jul. 2012.

[113] W. Cai *et al.*, "Synthesis of bulk-size transparent gadolinium oxide–polymer nanocomposites for gamma ray spectroscopy," *J. Mater. Chem. C*, vol. 1, no. 10, pp. 1970–1976, 2013.

[114] Z. Chen *et al.*, "Permeation and optical properties of YAG:Er^{3+} fiber membrane scintillators prepared by novel sol–gel/electrospinning method," *J. Sol-Gel Sci. Technol.*, vol. 83, no. 1, pp. 35–43, Jul. 2017.

[115] W. Chen and J. Zhang, "Using nanoparticles to enable simultaneous radiation and photodynamic therapies for cancer treatment," *J. Nanosci. Nanotechnol.*, vol. 6, no. 4, pp. 1159–1166, Apr. 2006.

[116] A.-L. Bulin *et al.*, "X-ray-induced singlet oxygen activation with nanoscintillator-coupled porphyrins," *J. Phys. Chem. C*, vol. 117, no. 41, pp. 21583–21589, Oct. 2013.

[117] R. Chouikrat *et al.*, "A photosensitizer lanthanide nanoparticle formulation that induces singlet oxygen with direct light excitation, but not by photon or X-ray energy transfer," *Photochem. Photobiol.*, vol. 93, no. 6, pp. 1439–1448, Nov. 2017.

[118] A.-L. Bulin, A. Vasil'ev, A. Belsky, D. Amans, G. Ledoux, and C. Dujardin, "Modelling energy deposition in nanoscintillators to predict the efficiency of the X-ray-induced photodynamic effect," *Nanoscale*, vol. 7, no. 13, pp. 5744–5751, 2015.

[119] N. Y. Morgan, G. Kramer-Marek, P. D. Smith, K. Camphausen, and J. Capala, "Nanoscintillator conjugates as photodynamic therapy-based radiosensitizers: Calculation of required physical parameters," *Radiat. Res.*, vol. 171, no. 2, pp. 236–244, Feb. 2009.

[120] H. Chen *et al.*, "Nanoscintillator-mediated X-ray inducible photodynamic therapy for *in vivo* cancer treatment," *Nano Lett.*, vol. 15, no. 4, pp. 2249–2256, Apr. 2015.

[121] J. Bárta, V. Čuba, M. Pospíšil, V. Jarý, and M. Nikl, "Radiation-induced preparation of pure and Ce-doped lutetium aluminium garnet and its luminescent properties," *J. Mater. Chem.*, vol. 22, no. 32, pp. 16590–16597, 2012.

[122] A. Kamkaew, F. Chen, Y. Zhan, R. L. Majewski, and W. Cai, "Scintillating nanoparticles as energy mediators for enhanced photodynamic therapy," *ACS Nano*, vol. 10, no. 4, pp. 3918–3935, Apr. 2016.

[123] S. E. Derenzo, M. J. Weber, and M. K. Klintenberg, "Temperature dependence of the fast, near-band-edge scintillation from CuI, HgI_2, PbI_2, ZnO:Ga and CdS:In," *Nucl. Instrum. Methods Phys. Res. A, Accel. Spectrom. Detect. Assoc. Equip.*, vol. 486, pp. 214–219, Jun. 2002.

[124] H. Burešová *et al.*, "Preparation and luminescence properties of ZnO:Ga—Polystyrene composite scintillator," *Opt. Exp.*, vol. 24, no. 14, pp. 15289–15298, Jul. 2016.

[125] A. Hospodková *et al.*, "InGaN/GaN multiple quantum well for fast scintillation application: Radioluminescence and photoluminescence study," *Nanotechnology*, vol. 25, no. 45, p. 455501, 2014.

[126] A. W. Achtstein *et al.*, "p-state luminescence in CdSe nanoplatelets: Role of lateral confinement and a longitudinal optical phonon bottleneck," *Phys. Rev. Lett.*, vol. 116, no. 11, p. 116802, Mar. 2016.

[127] Z. Xie *et al.*, "Ultracompact X-ray dosimeter based on scintillators coupled to a nano-optical antenna," *Opt. Lett.*, vol. 42, no. 7, pp. 1361–1364, Apr. 2017.

[128] M.-È. Delage, M.-È. Lecavalier, È. Cloutier, D. Larivière, C. N. Allen, and L. Beaulieu, "Robust shell passivation of CdSe colloidal quantum dots to stabilize radioluminescence emission," *AIP Adv.*, vol. 6, no. 10, p. 105011, Oct. 2016.

[129] S. Naskar *et al.*, "Photoluminescent Aerogels from Quantum Wells," *Chem. Mater.*, vol. 28, no. 7, pp. 2089–2099, Apr. 2016.

[130] W. Walravens *et al.*, "Chemically triggered formation of two-dimensional epitaxial quantum dot superlattices," *ACS Nano*, vol. 10, no. 7, pp. 6861–6870, Jul. 2016.

[131] Z. Ning *et al.*, "Quantum-dot-in-perovskite solids," *Nature*, vol. 523, no. 7560, pp. 324–328, 2015.

[132] M. Nasilowski, B. Mahler, E. Lhuillier, S. Ithurria, and B. Dubertret, "Two-dimensional colloidal nanocrystals," *Chem. Rev.*, vol. 116, no. 18, pp. 10934–10982, Sep. 2016.

[133] K. Akihiro, T. Kenjiro, S. Yasuo, and M. Tsutomu, "Organometal halide perovskites as visible-light sensitizers for photovoltaic cells," *J. Amer. Chem. Soc.*, vol. 131, no. 17, pp. 6050–6051, Apr. 2009.

[134] S. Yakunin *et al.*, "Detection of X-ray photons by solution-processed lead halide perovskites," *Nature Photon.*, vol. 9, no. 7, pp. 444–449, May 2015.

[135] S. Yakunin *et al.*, "Detection of gamma photons using solution-grown single crystals of hybrid lead halide perovskites," *Nature Photon.*, vol. 10, no. 9, pp. 585–589, Jul. 2016.

[136] W. Heiss and C. Brabec, "X-ray imaging: Perovskites target X-ray detection," *Nature Photon.*, vol. 10, no. 5, pp. 288–289, Apr. 2016.

[137] H. Wei *et al.*, "Dopant compensation in alloyed $CH_3NH_3PbBr_{3-x}Cl_x$ perovskite single crystals for gamma-ray spectroscopy," *Nature Mater.*, vol. 16, no. 8, pp. 826–833, Jul. 2017.

[138] K. Shibuya, M. Koshimizu, Y. Takeoka, and K. Asai, "Scintillation properties of $(C_6H_{13}NH_3)_2PbI_4$: Exciton luminescence of an organic/inorganic multiple quantum well structure compound induced by 2.0 MeV protons," *Nucl. Instrum. Methods Phys. Res. B, Beam Interact. Mater. At.*, vol. 194, no. 2, pp. 207–212, Aug. 2002.

[139] H. Wei *et al.*, "Sensitive X-ray detectors made of methylammonium lead tribromide perovskite single crystals," *Nature Photon.*, vol. 10, no. 5, pp. 333–339, Mar. 2016.

[140] T. Kondo *et al.*, "Resonant third-order optical nonlinearity in the layered perovskite-type material $(C_6H_{13}NH_3)_2PbI_4$," *Solid State Commun.*, vol. 105, no. 8, pp. 503–506, Feb. 1998.

[141] D. Cortecchia, K. C. Lew, J.-K. So, A. Bruno, and C. Soci, "Cathodoluminescence of self-organized heterogeneous phases in multidimensional perovskite thin films," *Chem. Mater.*, vol. 29, no. 23, pp. 10088–10094, 2017.

[142] M. D. Birowosuto *et al.*, "X-ray scintillation in lead halide perovskite crystals," *Sci. Rep.*, vol. 6, no. 1, Dec. 2016, Art. no. 37254

[143] Y. Fang, H. Wei, Q. Dong, and J. Huang, "Quantification of re-absorption and re-emission processes to determine photon recycling efficiency in perovskite single crystals," *Nature Commun.*, vol. 8, Feb. 2017, Art. no. 14417.

[144] G. A. Dosovitskiy *et al.*, "First 3D-printed complex inorganic polycrystalline scintillator," *CrystEngComm*, vol. 19, no. 30, pp. 4260–4264, 2017.

[145] [Online]. Available: https://indico.cern.ch/event/388511/

[146] T. Fukuda and V. I. Chani, *Micro-Pulling-Down (μ-PD) and Related Growth Methods*, T. Fukuda and V. I. Chani, Eds. Berlin, Germany: Springer, 2007.

[147] B. Hautefeuille *et al.*, "Shaped crystal growth of Ce^{3+}-doped $Lu_{2(1-x)}Y_{2x}SiO_5$ oxyorthosilicate for scintillator applications by pulling-down technique," *J. Cryst. Growth*, vol. 289, no. 1, pp. 172–177, 2006.

[148] H. Farhi *et al.*, "Fiber single crystal growth by LHPG technique and optical characterization of Ce^{3+}-doped Lu_2SiO_5," *Opt. Mater.*, vol. 30, no. 9, pp. 1461–1467, 2007.

[149] A. Yoshikawa and V. Chani, "Growth of optical crystals by the micro-pulling-down method," *MRS Bull.*, vol. 34, no. 4, pp. 266–270, Apr. 2009.

[150] P. Lecoq, "Metamaterials for novel X- or γ-ray detector designs," in *Proc. Conf. Rec. IEEE Nucl. Sci. Symp.*, Oct. 2008, pp. 1405–1409.

[151] E. Auffray, D. Abler, P. Lecoq, and G. Mavromanolakis, "Dual readout with PWO crystals and LuAG crystal scintillating fibers," *IEEE Trans. Nucl. Sci.*, vol. 57, no. 3, pp. 1454–1459, Jun. 2010.

[152] M. Lucchini *et al.*, "Test beam results with LuAG fibers for next-generation calorimeters," *J. Instrum.*, vol. 8, no. 10, p. P10017, 2013.

[153] A. Benaglia *et al.*, "Test beam results of a high granularity LuAG fibre calorimeter prototype," *J. Instrum.*, vol. 11, no. 5, p. P05004, May 2016.

[154] [Online]. Available: http://www.agence-nationale-recherche.fr/Projet-ANR-10-BLAN-0947

[155] [Online]. Available: https://intelum.web.cern.ch

[156] C. Dujardin *et al.*, "LuAG:Ce fibers for high energy calorimetry," *J. Appl. Phys.*, vol. 108, no. 1, p. 013510, 2010.

[157] X. Xu *et al.*, "Ce-doped LuAG single-crystal fibers grown from the melt for high-energy physics," *Acta Mater.*, vol. 67, pp. 232–238, Apr. 2014.

[158] V. Kononets *et al.*, "Growth of long undoped and Ce-doped LuAG single crystal fibers for dual readout calorimetry," *J. Cryst. Growth*, vol. 435, pp. 31–36, Feb. 2016.

[159] A. Vedda *et al.*, "Ce^{3+}-doped fibers for remote radiation dosimetry," *Appl. Phys. Lett.*, vol. 85, no. 26, pp. 6356–6358, Dec. 2004.

[160] A. Vedda *et al.*, "Insights into microstructural features governing Ce^{3+} luminescence efficiency in sol-gel silica glasses," *Chem. Mater.*, vol. 18, no. 26, pp. 6178–6185, Dec. 2006.

[161] I. Veronese *et al.*, "Infrared luminescence for real time ionizing radiation detection," *Appl. Phys. Lett.*, vol. 105, no. 6, p. 061103, Aug. 2014.

[162] F. Cova *et al.*, "Ippolito, and A. Vedda, "Optical properties and radiation hardness of Pr-doped sol-gel silica: Influence of fiber drawing process," *J. Lumin.*, vol. 192, pp. 661–667, Dec. 2017.

[163] F. Cova *et al.*, "Radiation hardness of Ce-doped sol-gel silica fibers for high energy physics applications," *Opt. Lett.*, vol. 43, no. 4, pp. 903–906, Feb. 2018.

[164] A. Yoshikawa *et al.*, "Phase identification of $Al_2O_3/RE_3Al_5O_{12}$ and $Al_2O_3/REAlO_3$ (RE=Sm–Lu, Y) eutectics," *J. Cryst. Growth*, vol. 218, no. 1, pp. 67–73, Sep. 2000.

[165] J. LLorca and V. M. Orera, "Directionally solidified eutectic ceramic oxides," *Prog. Mater. Sci.*, vol. 51, no. 6, pp. 711–809, 2006.

[166] S. Kurosawa *et al.*, "Growth and optical properties of LiF/LaF_3 eutectic crystals," *J. Eur. Ceram. Soc.*, vol. 34, no. 9, pp. 2111–2115, Aug. 2014.

[167] K. Nishimoto *et al.*, "Crystal growth of $LiF/LiYF_4$ eutectic crystals and their luminescent properties," *J. Eur. Ceram. Soc.*, vol. 34, no. 9, pp. 2117–2121, Aug. 2014.

[168] Y. Ohashi, N. Yasui, Y. Yokota, A. Yoshikawa, and T. Den, "Submicron-diameter phase-separated scintillator fibers for high-resolution X-ray imaging," *Appl. Phys. Lett.*, vol. 102, no. 5, p. 051907, Feb. 2013.

[169] N. Yasui, T. Kobayashi, Y. Ohashi, and T. Den, "Phase-separated CsI-NaCl scintillator grown by the Czochralski method," *J. Cryst. Growth*, vol. 399, pp. 7–12, Aug. 2014.

[170] A. Koch, C. Raven, P. Spanne, and A. Snigirev, "X-ray imaging with submicrometer resolution employing transparent luminescent screens," *J. Opt. Soc. Amer. A, Opt. Image Sci.*, vol. 15, no. 7, pp. 1940–1951, Jul. 1998.

[171] Y. Zorenko *et al.*, "Single crystalline film scintillators based on the orthosilicate, perovskite and garnet compounds," *IEEE Trans. Nucl. Sci.*, vol. 59, no. 5, pp. 2260–2268, Oct. 2012.

[172] P.-A. Douissard *et al.*, "A novel epitaxially grown LSO-based thin-film scintillator for micro-imaging using hard synchrotron radiation," *J. Synchrotron Radiat.*, vol. 17no. 5, pp. 571–583, Sep. 2010.

[173] A. García-Murillo *et al.*, "Elaboration and scintillation properties of Eu^{3+}-doped Gd_2O_3 and Lu_2O_3 sol–gel films," *Nucl. Instrum. Methods Phys. Res. A, Accel. Spectrom. Detect. Assoc. Equip.*, vol. 486, nos. 1–2, pp. 181–185, Jun. 2002.

[174] T. Martin *et al.*, "New high stopping power thin scintillators based on Lu_2O_3 and $Lu_3Ga_{5-x}In_xO_{12}$ for high resolution X-ray imaging," *IEEE Trans. Nucl. Sci.*, vol. 59, no. 5, pp. 2269–2274, Oct. 2012.

[175] F. Riva, T. Martin, P. A. Douissard, and C. Dujardin, "Single crystal lutetium oxide thin film scintillators for X-ray imaging," *J. Instrum.*, vol. 11, no. 10, p. C10010, Oct. 2016.

[176] F. Riva, P.-A. Douissard, T. Martin, F. Carlá, Y. Zorenko, and C. Dujardin, "Epitaxial growth of gadolinium and lutetium-based aluminum perovskite thin films for X-ray micro-imaging applications," *CrystEngComm*, vol. 18, no. 4, pp. 608–615, 2016.

[177] M. S. Alekhin *et al.*, "Stimulated scintillation emission depletion X-ray imaging," *Opt. Express*, vol. 25, no. 2, pp. 654–669, 2017.

[178] M. S. Alekhin *et al.*, "STED properties of Ce^{3+}, Tb^{3+}, and Eu^{3+} doped inorganic scintillators," *Opt. Express*, vol. 25, no. 2, pp. 1251–1261, 2017.

[179] A. Pereira, T. Martin, M. Levinta, and C. Dujardin, "Low-absorption, multi-layered scintillating material for high resolution real-time X-ray beam analysis," *J. Mater. Chem. C*, vol. 3, no. 19, pp. 4954–4959, 2015.

[180] A. N. Vasil'ev and A. V. Gektin, "Multiscale approach to estimation of scintillation characteristics," *IEEE Trans. Nucl. Sci.*, vol. 61, no. 1, pp. 235–245, Feb. 2014.

[181] A. N. Vasil'ev, "Microtheory of scintillation in crystalline materials," in *Proc. Int. Conf. Eng. Scintillation Mater. Radiat. Technol.* Berlin, Germany: Springer, 2017, pp. 3–34.

[182] H. Huang, Q. Li, X. Lu, Y. Qian, Y. Wu, and R. T. Williams, "Role of hot electron transport in scintillators: A theoretical study," *Phys. Status Solidi, Rapid Res. Lett.*, vol. 10, no. 10, pp. 762–768, 2016.

[183] M. P. Prange, L. W. Campbell, D. Wu, F. Gao, and S. Kerisit, "Calculation of energy relaxation rates of fast particles by phonons in crystals," *Phys. Rev. B, Condens. Matter*, vol. 91, no. 10, p. 104305, 2015.

[184] M. P. Prange, L. W. Campbell, and S. Kerisit, "Electron-phonon scattering rates in complex polar crystals," *Phys. Rev. B, Condens. Matter*, vol. 96, no. 10, p. 104307, 2017.

[185] J. Singh, R. T. Williams, A. Koblov, and D. Surovtseva, "Effect of time-dependent local excitonic concentration in the track on nonproportionality in light yield of inorganic scintillators," *IEEE Trans. Nucl. Sci.*, vol. 61, no. 1, pp. 252–256, Feb. 2014.

[186] X. Lu *et al.*, "Coupled rate and transport equations modeling proportionality of light yield in high-energy electron tracks: CsI at 295 K and 100 K; CsI:Tl at 295 K," *Phys. Rev. B, Condens. Matter*, vol. 92, no. 11, p. 115207, 2015.

[187] Q. Li, X. Lu, and R. T. Williams, "Toward a user's toolkit for modeling scintillator non-proportionality and light yield," *Proc. SPIE, Hard X-Ray, Gamma-Ray, Neutron Detect. Phys. XVI*, vol. 9213, p. 92130K, Sep. 2014, doi: 10.1117/12.2063468.

[188] M. Prange, D. Wu, Y. Xie, L. W. Campbell, F. Gao, and S. Kerisit, "Radiation response of inorganic scintillators: Insights from Monte Carlo simulations," *Proc. SPIE, Hard X-Ray, Gamma-Ray, Neutron Detect. Phys. XVI*, vol. 9213, p. 92130L, Sep. 2014, doi: 10.1117/12.2063818.

[189] S. Kerisit, Z. Wang, R. T. Williams, J. Q. Grim, and F. Gao, "Kinetic Monte Carlo simulations of scintillation processes in NaI(Tl)," *IEEE Trans. Nucl. Sci.*, vol. 61, no. 2, pp. 860–869, Apr. 2014.

[190] M. P. Prange, Y. Xie, L. W. Campbell, F. Gao, and S. Kerisit, "Monte Carlo simulation of electron thermalization in scintillator materials: Implications for scintillator nonproportionality," *J. Appl. Phys.*, vol. 122, no. 23, p. 234504, 2017.

[191] M. Moszyński *et al.*, "Energy resolution and slow components in undoped CsI crystals," *IEEE Trans. Nucl. Sci.*, vol. 63, no. 2, pp. 459–466, Apr. 2016.

[192] S. A. Payne, S. Hunter, L. Ahle, N. J. Cherepy, and E. Swanberg, "Nonproportionality of scintillator detectors. III. Temperature dependence studies," *IEEE Trans. Nucl. Sci.*, vol. 61, no. 5, pp. 2771–2777, Oct. 2014.

[193] S. A. Payne, "Nonproportionality of scintillator detectors. IV. Resolution contribution from delta-rays," *IEEE Trans. Nucl. Sci.*, vol. 62, no. 1, pp. 372–380, Feb. 2015.

[194] P. R. Beck, S. A. Payne, S. Hunter, L. Ahle, N. J. Cherepy, and E. L. Swanberg, "Nonproportionality of scintillator detectors. V. Comparing the gamma and electron response," *IEEE Trans. Nucl. Sci.*, vol. 62, no. 3, pp. 1429–1436, Jun. 2015.

[195] A. Gektin, S. Gridin, S. Vasyukov, A. Vasil'ev, A. Belsky, and N. Shiran, "Effect of the activator impurity on the scintillation yield in alkali-halide crystals," *Phys. Status Solidi B*, vol. 252, no. 2, pp. 380–385, 2015.

[196] S. Gridin, A. Belsky, C. Dujardin, A. Gektin, N. Shiran, and A. Vasil'ev, "Kinetic model of energy relaxation in CsI:A (A = Tl and In) scintillators," *J. Phys. Chem. C*, vol. 119, no. 35, pp. 20578–20590, Sep. 2015.

[197] S. Gridin, A. N. Vasil'ev, A. Belsky, N. Shiran, and A. Gektin, "Excitonic and activator recombination channels in binary halide scintillation crystals," *Phys. Status Solidi B*, vol. 251, no. 5, pp. 942–949, 2014, doi: 10.1002/pssb.201350234.

[198] A. Gektin, "Fluctuations of ionizing particle track structure and energy resolution of scintillators," *Funct. Mater.*, vol. 24, no. 4, pp. 621–627, 2017.

[199] S. Omelkov, V. Nagirnyi, A. N. Vasil'ev, and M. Kirm, "New features of hot intraband luminescence for fast timing," *J. Lumin.*, vol. 176, pp. 309–317, Aug. 2016.

[200] A. N. Vasil'ev and R. V. Kirkin, "Emission spectrum of intraband luminescence for single parabolic band under excitation of wide-band-gap insulators by ionizing radiation and particles," *Phys. Wave Phenomena*, vol. 23, no. 3, pp. 186–191, Jul. 2015.

[201] [Online]. Available: http://cordis.europa.eu/project/rcn/110957_en.html

[202] [Online]. Available: http://fastcost.web.cern.ch/fast-cost/

[203] A. V. Gektin, A. N. Belsky, and A. N. Vasil'ev, "Scintillation efficiency improvement by mixed crystal use," *IEEE Trans. Nucl. Sci.*, vol. 61, no. 1, pp. 262–270, Feb. 2014.

[204] A. Belsky, A. Gektin, S. Gridin, and A. N. Vasil'ev, "Electronic and optical properties of scintillators based on mixed ionic crystals," in *Engineering of Scintillation Materials and Radiation Technologies*. Berlin, Germany: Springer, 2017, pp. 63–82.

[205] T. Demkiv *et al.*, "Intrinsic luminescence of SrF_2 nanoparticles," *J. Lumin.*, vol. 190, pp. 10–15, Oct. 2017.

[206] V. Vistovskyy *et al.*, "Modeling of X-ray excited luminescence intensity dependence on the nanoparticle size," *Radiat. Meas.*, vol. 90, pp. 174–177, Jul. 2016.

[207] [Online]. Available: http://www.aflowlib.org/

[208] W. Setyawan, R. M. Gaume, S. Lam, R. S. Feigelson, and S. Curtarolo, "High-throughput combinatorial database of electronic band structures for inorganic scintillator materials," *ACS Combinat. Sci.*, vol. 13, no. 4, pp. 382–390, Jul. 2011.

[209] C. Bouzidi, K. Horchani-Naifer, Z. Khadraoui, H. Elhouichet, and M. Ferid, "Synthesis, characterization and DFT calculations of electronic and optical properties of $CaMoO_4$," *Phys. B, Condens. Matter*, vol. 497, pp. 34–38, Sep. 2016.

[210] A. Chaudhry, R. Boutchko, S. Chourou, G. Zhang, N. Grønbech-Jensen, and A. Canning, "First-principles study of luminescence in Eu^2+-doped inorganic scintillators," *Phys. Rev. B, Condens. Matter*, vol. 89, no. 15, p. 155105, Apr. 2014.

[211] D. Wu, M. P. Prange, F. Gao, and S. Kerisit, "First-principles search for efficient activators for LaI_3," *J. Lumin.*, vol. 176, pp. 227–234, Aug. 2016.

[212] M. H. Du, "Chemical trends of electronic and optical properties of ns^2 ions in halides," *J. Mater. Chem. C*, vol. 2, no. 24, pp. 4784–4791, 2014.

[213] M.-H. Du, "Using DFT methods to study activators in optical materials," *ECS J. Solid State Sci. Technol.*, vol. 5, no. 1, pp. R3007–R3018, Aug. 2016.

[214] A. Alkauskas, Q. Yan, and C. G. Van de Walle, "First-principles theory of nonradiative carrier capture via multiphonon emission," *Phys. Rev. B, Condens. Matter*, vol. 90, no. 7, p. 075202, Aug. 2014.

[215] A. Alkauskas, M. D. McCluskey, and C. G. Van de Walle, "Tutorial: Defects in semiconductors—Combining experiment and theory," *J. Appl. Phys.*, vol. 119, no. 18, p. 181101, May 2016.

[216] D. N. Krasikov, A. V. Scherbinin, A. A. Knizhnik, A. N. Vasiliev, B. V. Potapkin, and T. J. Sommerer, "Theoretical analysis of non-radiative multiphonon recombination activity of intrinsic defects in CdTe," *J. Appl. Phys.*, vol. 119, no. 8, p. 085706, Feb. 2016.

[217] P. Lecoq, A. Gektin, and M. Korzhik, *Inorganic Scintillators for Detector Systems*, 2nd ed. Springer, 2017.